

Completing the set of *h/E(spl)* cyclic genes in zebrafish: *her12* and *her15* reveal novel modes of expression and contribute to the segmentation clock

Sunita S. Shankaran^{a,1,3}, Dirk Sieger^{a,3}, Christian Schröter^b, Carmen Czepe^{a,2},
Marie-Christin Pauly^a, Mary A. Laplante^c, Thomas S. Becker^c,
Andrew C. Oates^b, Martin Gajewski^{a,*}

^a Institute for Genetics, University of Cologne, Zùlpicher Str. 47, 50674 Cologne, Germany

^b Max Planck Institute for Molecular Cell Biology and Genetics, Pfotenhauerstr 108, 01307 Dresden, Germany

^c Sars International Centre for Marine Molecular Biology at the University of Bergen, Thormoehlensgate 55, 5008 Bergen, Norway

Received for publication 26 September 2006; revised 19 December 2006; accepted 4 January 2007

Available online 9 January 2007

Abstract

Somitogenesis is the key developmental process that lays down the framework for a metameric body in vertebrates. Somites are generated from the un-segmented presomitic mesoderm (PSM) by a pre-patterning process driven by a molecular oscillator termed the segmentation clock. The Delta–Notch intercellular signaling pathway and genes belonging to the *hairy (h)* and *Enhancer of split (E(spl))*-related (*h/E(spl)*) family of transcriptional repressors are conserved components of this oscillator. A subset of these genes, called cyclic genes, is characterized by oscillating mRNA expression that sweeps anteriorly like a wave through the embryonic PSM. Periodic transcriptional repression by *h/E(spl)* proteins is thought to provide a critical part of a negative feedback loop in the oscillatory process, but it is an open question how many cyclic *h/E(spl)* genes are involved in the somitogenesis clock in any species, and what distinct roles they might play. From a genome-wide search for *h/E(spl)* genes in the zebrafish, we previously estimated a total of five cyclic members. Here we report that one of these, the *mHes5* homologue *her15* actually exists as a very recently duplicated gene pair. We investigate the expression of this gene pair and analyse its regulation and activity in comparison to the paralogous *her12* gene, and the other cyclic *h/E(spl)* genes in the zebrafish. The *her15* gene pair and *her12* display novel and distinct expression features, including a caudally restricted oscillatory domain and dynamic stripes of expression in the rostral PSM that occur at the future segmental borders. *her15* expression stripes demarcate a unique two-segment interval in the rostral PSM. Mutant, morpholino, and inhibitor studies show that *her12* and *her15* expression in the PSM is regulated by Delta–Notch signaling in a complex manner, and is dependent on *her7*, but not *her1* function. Morpholino-mediated *her12* knockdown disrupts cyclic gene expression, indicating that it is a non-redundant core component of the segmentation clock. Over-expression of *her12*, *her15* or *her7* disrupts cyclic gene expression and somite border formation, and structure function analysis of *Her7* indicates that DNA binding, but not Groucho-recruitment seems to be important in this process. Thus, the zebrafish has five functional cyclic *h/E(spl)* genes, which are expressed in a distinct spatial configuration. We propose that this creates a segmentation oscillator that varies in biochemical composition depending on position in the PSM.

© 2007 Elsevier Inc. All rights reserved.

Keywords: Cyclic *h/E(spl)* genes; Segmentation clock; Somitogenesis; bHLH transcription factor

Introduction

Somite segmentation in vertebrate embryos is regulated by a clock mechanism in the presomitic mesoderm (PSM) that becomes evident on a molecular level in the form of coordinated waves of transcriptional oscillations. Most of the genes implicated in the segmentation clock belong to the Delta–Notch signaling cascade or its PSM target genes, the majority of which encode bHLH transcriptional repressors of the *her/hes*/

* Corresponding author. Fax: +49 221 470 5975.

E-mail address: martin.gajewski@uni-koeln.de (M. Gajewski).

¹ Present address: Adolf-Butenandt-Institute, Department of Biochemistry, Schillerstrasse 44, 80336 Munich, Germany.

² Present address: Institute of Animal Breeding and Genetics University of Veterinary Medicine, Veterinärplatz 1, 1210 Vienna, Austria.

³ These authors contributed equally.

esr (*h/E(spl)*) family (reviewed by Bessho and Kageyama, 2003; Rida et al., 2004; Giudicelli and Lewis, 2004). In all species examined, binding of the cell-surface ligand Delta to the extracellular domain of Notch on a neighboring cell results in the cleavage and translocation of the intracellular domain to the nucleus, where it activates transcription as part of a complex with CSL transcription factors (del Barco Barrantes et al., 1999; Sieger et al., 2003; Morimoto et al., 2005; Huppert et al., 2005). In zebrafish, this signaling event is required for the maintenance of *h/E(spl)* PSM expression levels (Oates et al., 2005), and may be responsible for maintaining the synchrony of neighboring PSM cells (Jiang et al., 2000; Horikawa et al., 2006; Masamizu et al., 2006). In contrast, *H/E(spl)* family proteins are thought to comprise a key negative-feedback step in the generation of cell-autonomous oscillations in mice and zebrafish because of their activity as transcriptional repressors (Holley et al., 2002; Oates and Ho, 2002; Gajewski et al., 2003; Bessho et al., 2003; Hirata et al., 2004; Kawamura et al., 2005), a role that is supported by mathematical modeling of the process (Lewis, 2003). However, this necessarily simplistic view does not yet explain many striking experimental observations in growing embryos.

Multiple *h/E(spl)* genes are expressed in the PSM of each vertebrate embryo, but not all exhibit dynamic “cyclic” expression waves (Takke et al., 1999; Pasini et al., 2004), nor do all orthologues of a given cyclic *h/E(spl)* gene show cyclic expression in other species (Leve et al., 2001; Gajewski and Voolstra, 2002; Gajewski et al., 2006). Furthermore, not all cyclic *h/E(spl)* genes yield somite phenotypes when knocked out or down. For example, mutations in the mouse cyclic *Hes7* gene exhibit a strong somitogenic phenotype, with a complete disruption of oscillatory gene expression (Bessho et al., 2003), whereas the cyclic *Hes1* and *Hes5* gene mutants show no effect on somitogenesis or oscillatory processes (Ishibashi et al., 1995; Jensen et al., 2000; Jouve et al., 2000). Studies of zebrafish *h/E(spl)* genes suggest that genetic redundancy masks some essential functions of family members (Oates and Ho, 2002; Pasini et al., 2004; Sieger et al., 2004, 2006). The ability of the *H/E(spl)* proteins to form DNA-binding homo- and heterodimers (Leimeister et al., 2000) further complicates analysis and interpretation of their function in somitogenesis and the segmentation clock. Thus, although all vertebrates so far examined rely on cyclic *h/E(spl)* genes for somitogenesis, each of these *h/E(spl)* genes appears to have unique properties, and play distinct roles in the process. In no species do we understand in detail the functional interactions and characteristics of such a *h/E(spl)* “network” (Leimeister et al., 2000). In order to achieve this, we first need a complete list of cyclic *h/E(spl)* genes from a given species, and a description of their mutant and over-expression phenotypes.

We previously carried out a genome-wide search for *h/E(spl)* genes in zebrafish and identified three additional oscillating genes, two of which we have previously described: *her11*, a *mHes7* homologue (Sieger et al., 2004), and *her12*, a *mHes5* homologue (Gajewski et al., 2006). Here we complete this genome-wide search in the almost finished zebrafish sequence by presenting the expression, regulation and functional analysis of a very recently duplicated gene pair homologous to *mHes5*

termed *her15a* and *her15b*. The *her15b* duplicate is uniquely marked by the insertion of a retroviral enhancer trap 5' to the exons. Comparison of the different *mHes5* homologues reveals that *her15* and *her12* show unique expression features and differential regulation via Delta–Notch compared to the other oscillating *h/E(spl)* genes *her1*, *her7* and *her11* (Gajewski et al., 2003; Henry et al., 2002; Holley et al., 2000, 2002; Oates and Ho, 2002; Sieger et al., 2004). During somite formation, they are expressed in novel, regionally restricted oscillatory domains in the PSM. Functional analysis of *her15* and *her12* suggests involvement in the core clock mechanism, albeit to different extents, and thus reveals a direct role in the process of somite formation for members of this subfamily of *h/E(spl)*-related genes. Combining these findings, we propose a *h/E(spl)* “code” for the PSM that suggests differential sets of *H/E(spl)* proteins define sub-regions of the oscillatory field of cells.

Materials and methods

Fish rearing, embryo collection, wild type and mutant strains

The adult fish were raised and maintained at 28.5 °C at 14-h light /10-h dark cycle. Embryos were collected by natural spawning and staged according to Kimmel et al. (1995). The wild type strain was used from a local commercial supplier and the used mutant strains *after eight* (*aet*^{tg249}), *beamter* (*bed*^{tm98}), *deadly seven* (*des*^{tp37}) and *fused somite* (*fss*^{te314a}) have been previously described (Julich et al., 2005; Holley et al., 2000, 2002; Nikaido et al., 2002; van Eeden et al., 1996).

Analysis of her15 gene pair

The sequence of primer pairs used to identify the two *her15* gene loci from wild type *AB strain genomic DNA were as follows: shared outer *pher15in1R* (5'-GAA GCG TCA GAT GTA TTC CAG-3'); shared inner *pher15ex1R* (5'-TGG AAA GCT TGG AGT ATT CAG-3'), with *her15a* locus specific outer *her15.1–441F* (5'-TCA GTG CGA TAA GGT GTT TC-3') and inner *her15.1–517F* (5'-CCA TCT GTC CTT ATC AGT GC-3') or *her15b* locus-specific outer *her15.2–490F* (5'-TTG CAA TCT TTC TCG TAA ATG-3') and inner *her15.2–601F* (5'-TGT AAT GAT TGT GGT AAG ATC AAG-3'). Reaction conditions are available upon request.

Probe design and whole mount in situ hybridisation

The sequences of *her12* and *her15a* are deposited under Accession Numbers AY426713 and AY576277, respectively, in the GenBank database. Two gene copies exist for *her4* (Sieger et al., 2004). Both genes, *her4.1* and *her4.2*, are highly similar and we cannot distinguish between both copies. Therefore we refer to them as *her4*, but the probe for *in situ* hybridisation is generated from the *her4.1* template. In detail, the *her4.1*, *her12* and *her15* *in situ* probe was PCR-amplified using the following primer sets namely *her4.1*-for (5'-GTG ATG CTT GGA AAT CAA T-3') and T7-*her4.1*-rev (5'-TAA TAC GAC TCA CTA TAG GGT GCA GAT GTT GTC CAT CTT CG-3'), *her12*-for (5'-ATG GCA CCC CAC TCA GCC ACA CTC GCC TCC-3') and T7-*her12*-rev (5'-TAA TAC GAC TCA CTA TAG GGT CTC CAG ACG GCC C-3'), T3-*her15up* (5'-AAT TAA CCC TCA CTA AAG GGC TCC TGC GTA TAT G-3') and T7-*her15down* (5'-TAA TAC GAC TCA CTA TAG GGT CTC CAG AGC GGA G-3'), at an annealing temperature of 55 °C. The PCR template was used for *in vitro* transcription of a digoxigenin labelled RNA-probe (Roche), enabling subsequent detection by an anti-digoxigenin antibody coupled to alkaline phosphatase and using BM purple (Roche). *titin* is described in Oates et al. (2005). For double *in situ* hybridisation, fluorescein-labelled *myoD* and *her7* probes were generated and detected with an anti-fluorescein conjugate coupled to alkaline phosphatase using VectorRed (Linaris). Double *in situ* hybridisations were performed with both probes simultaneously but the antibody detection and

staining was done consecutively introducing a step to destroy the first alkaline phosphatase before detection and staining the second probe. The Hybridisation of the *in situ* probe(s) was usually performed at 65 °C, using a programmable liquid handling system (InsituPro, Intavis) described by Plickert et al. (1997). Whole-mount and flat-mounted embryos were prepared in methylcellulose and glycerol, respectively. Whole-mount preparations were observed under a stereomicroscope (Leica) and digitally photographed (Axiocam, Zeiss). An Axioplan2 microscope (Zeiss) was used for the analysis of flat-mounted embryos.

Morpholino oligonucleotide design, misexpression constructs and injections

Morpholino oligonucleotides (Mo) were synthesized by Gene Tools and injected into 1- to 2-cell stage zebrafish embryos. The injection solution consisted of 0.6 mM of the respective Mo, 0.2% phenol red and 0.1 M KCl. The sequences of *her1* Mo, *her7* Mo and *Su(H)* Mo are as described (Gajewski et al., 2003; Sieger et al., 2003). The sequences of the *her12* Mo are: 5'-AGG CGA GTG TGG CTG AGT GGG GTG C-3' (*her12*-ORF) and 5'-CGA ATG CAT GTG ACA GGG AGG TCA T-3' (*her12*-control).

For misexpression of *her11*, *her12* and *her15*, the respective ORF sequence was amplified with respective primers (*her11*-*Clal*-for: 5'-AGA GAG ATC GAT ATG AAG AGC ACA CCG ACT TTC-3', *her11*-*XhoI*-rev: 5'-GAG AGA CTC GAG GAT TCA ACT CAT TTA TTC CAC-3', *her12*-*XhoI*-for: 5'-ATC TCG AGC TGT TCG AGC ACA GAC ATG G-3', *her12*-*XbaI*-rev: 5'-AGT CTA GAC TCA GGG TTG TCA GTC CAC A-3', *her15*-*Clal*-for: 5'-GCATCG ATA TGG CTC CTG CGT ATA TGA C-3', *her15*-*XhoI*-rev: 5'-TAA CTC GAG CTA CCA GGG TCT CCA GAG-3') containing restriction sites for *Clal*, *XhoI* and *XbaI* as indicated. The PCR product was gel purified, digested and cloned into the pCS2⁺ vector (Turner and Weintraub, 1994). To allow the generation of *her7* mRNA for microinjection, the *her7* coding sequence was amplified using primers *her7*ATG: 5'-CGG GAT CCC ACC ATG AAA ATC CTG GCA CAG ACT-3' and *her7*TAA: 5'-CCG CTC GAG TTA AGG CCA AGG TCT CCA GAC-3', restricted with *Bam*HI and *Xho*I, and ligated into a *Bam*HI/*Xho*I-cut pCS2⁺ expression plasmid, to create pCS2⁺-*her7*. Mutant versions of *her7* lacking the N-terminal, basic DNA-binding region, and the C-terminal Groucho-binding peptide were created by amplifying from pGEM TEasy-*her7*cds with primers *her7*Δbas: 5'-CGG GAT CCC ACC ATG GAA AGG ATG AAC CGG AGT CTA-3' and *her7*TAA and *her7*Δwrp: 5'-CCG CTC GAG TTA AGT CTG GCT GGC TGG TTC T-3', respectively, restricting with *Bam*HI and *Xho*I, and ligating into *Bam*HI/*Xho*I-cut pCS2⁺ to create pCS2⁺-*her7*ΔBAS and pCS2⁺-*her7*ΔWRPW. To verify expression of the exogenous protein, an N-terminal Myc epitope fusion was constructed by amplifying from pGEM TEasy-*her7*cds with primers *her7*ATGEco: 5'-CGG AAT TCA ATG AAA ATC CTG GCA CAG ACT GA-3' and *her7*TAA, restricting with *Eco*RI and *Xho*I and ligating into *Eco*RI/*Xho*I-cut pCS2⁺MT to create pCS2⁺-Myc*her7*. All constructs were verified by sequencing both strands by the sequencing facility at the University of Cologne (*her11*-, *her12*-, *her15*- and *eGFP*-constructs) or by the SynSeq facility at Princeton University (*her7*-constructs).

As control for these functional studies a pCS2⁺-eGFP construct was used (kindly provided by the Lab of Jose Campos-Ortega). To control the binding of the different morpholinos, the 5'-sequences of the different genes were cloned upstream of eGFP in the same vector. Capped mRNA was made using the "message machine kit" (Ambion). Injections were carried out using an Eppendorf Femtojet and micromanipulator.

DAPT treatment was done as described to inhibit the cleavage of the intracellular domain of the Notch receptor by presenilin with a concentration of 100 μM (Geling et al., 2002).

Immunohistochemistry

The Myc and GFP epitopes were detected in whole mount embryos according to Bruce et al. (2001). The 9E10 anti-Myc monoclonal antibody was developed by J. M. Bishop and obtained from the Developmental Studies Hybridoma Bank under the auspices of the NICHD and maintained at the University of Iowa, Department of Biological Sciences, and the anti-GFP rabbit polyclonal antibody was from Molecular Probes, Eugene, Oregon. Anti-Myc and anti-GFP antibodies were used at 1:100 and 1:500 dilutions, respectively. Color development used the Vectastain kit (Vector Laboratories, CA).

Results

Evolutionary relationships of the *mHes5* homologues in fish

The *her12* and *her15* zebrafish *h/E(spl)* gene family members, together with *her2*, *her4.1* (formerly *her4*, Takke et al., 1999) and *her4.2*, belong to a subclass that is most similar to the cyclically expressed mouse *Hes5* gene (Dunwoodie et al., 2002; Gajewski and Voolstra, 2002; Sieger et al., 2004; Gajewski et al., 2006). They possess 2 exons each, and contain characteristic H/E(spl) protein domains, including the conserved basic-Helix I-Loop-Helix II, Orange domain and a WRPW motif at the C-terminus (Fig. 1A; reviewed by Davis and Turner, 2001). Alignment with members of the same subclass such as mouse *Hes5* and *Xenopus* *esr9* and *esr10*, shows sequence conservation between 46% and 58% (Fig. 1B; Gajewski et al., 2006; Li et al., 2003; Takebayashi et al., 1995). *her4.1* has been shown to play a role during late somitogenesis, whereas *her2* is expressed earlier in somitogenesis in the posterior halves of the 3 anterior-most somites, but not in the PSM (Pasini et al., 2004; Weizsäcker, 1994; Takke et al., 1999). *her12* has been found in all fish species analysed so far, while *her15* seems to be specific to zebrafish (Gajewski et al., 2006).

Blast searches of the current Ensembl zebrafish genome assembly 41 reveal two loci on Chr 11 with very high exon identity (99–100%) to our previously published *her15* sequence (AY576277). One, also known as *hes5* (ENS DARG00000054562) matches *her15* exactly, and we term this gene *her15a*. The other, termed *her15b* (ENS DARG00000054560), is predicted to lie approximately 12 kb away in a tail to tail orientation. The coding exons lie in a block of near-complete sequence identity (1730/1750 bp, 99%) extending approximately 170 bp 5' to the start codon and 805 bp 3' to the stop codon. The three substitutions in the coding region result only in a single change at residue Q114R (see Fig. 1, asterisk), which does not lie in any of the conserved domains of the *h/E(spl)* gene family. To test whether the conserved block was an artifact of assembly, we used PCR with primers targeted to the first exon and intron of the *her15* genes and a second set of primers targeted to locus-specific sequences outside the conserved block to amplify the respective regions from *AB wild type strain genomic DNA. Sequencing of the differently sized products revealed genomic fragments matching the Ensembl assembly (data not shown). Thus, the high sequence identity of the two genes indicates a very recent duplication event, and the near exact match of the predicted transcripts would prevent us from distinguishing between expression from the two loci by *in situ* hybridisation. However, the insertion of a retrovirus next to *her15b* provides independent evidence for the existence of the second *her15* paralogue, and may allow the detection of individual *her15* gene expression (see Fig. 3). We therefore refer to the sum of transcription from *her15a* and *her15b* as the expression of the *her15* gene pair.

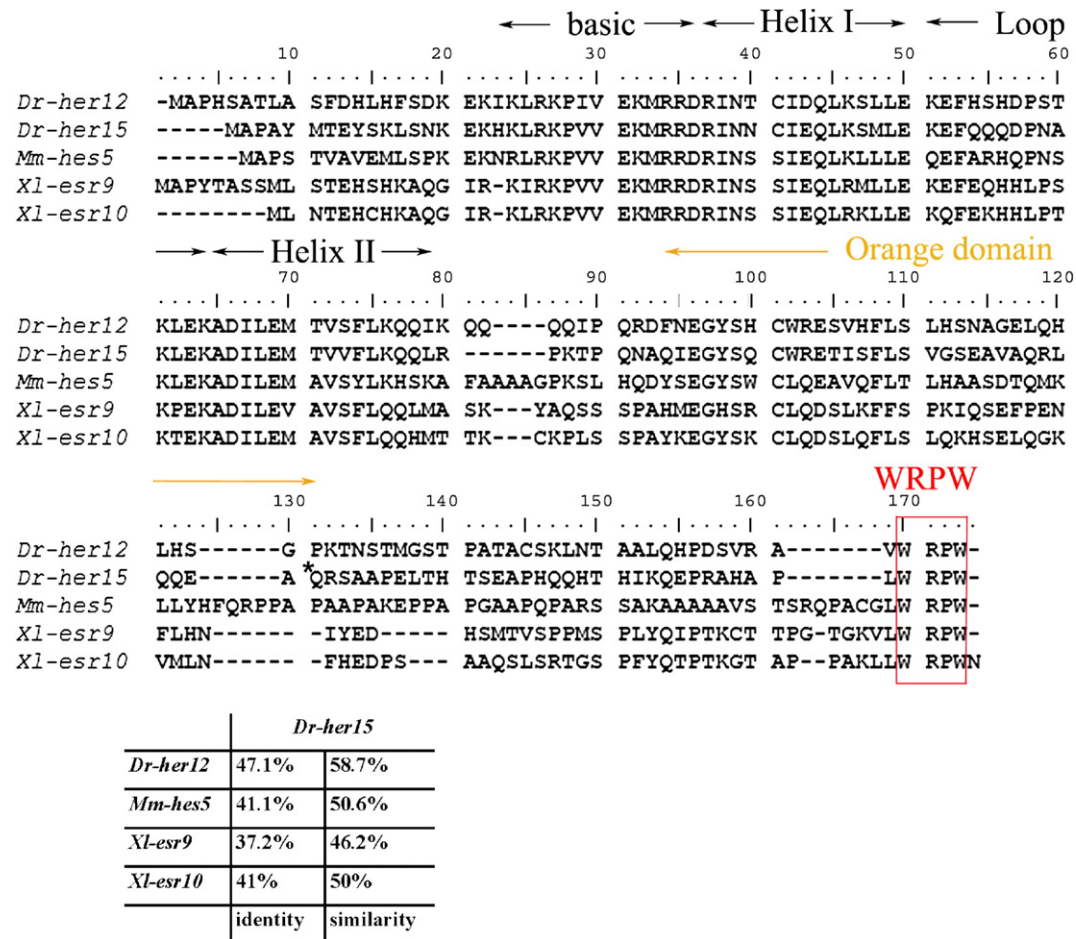


Fig. 1. Sequence analysis of *her15*. (A) Alignment of zebrafish *her15* with different *mHes5* homologues is shown. Positions of the different domains are indicated above the alignment. Dr, *Danio rerio*; Mm, *Mus musculus*; Xl, *Xenopus laevis*. (B) Table shows the different sequence similarities and identities of *her15* to other *mHes5* homologues. Position of the variant residue between *Her15a* and *Her15b* is shown with an asterisk.

Analysis of *her15* mRNA distribution reveals a novel cyclic expression pattern

her12 exhibits a cyclic expression domain from early somitogenesis stages that spatially and temporally resembles the posterior-most expression domains of *her1* and *her7* (Gajewski et al., 2003, 2006; Holley et al., 2000; Henry et al., 2002; Oates and Ho, 2002). Expression of a single *her15* gene in the CNS was reported previously (called *Hes5* in Bae et al., 2005), but expression in the PSM and tail bud has not been characterized. mRNA transcripts from the *her15* gene pair are first detected during late epiboly stages in the margin, but are excluded from the midline (Figs. 2A, B). The different width of expression around the epibolic margin in different embryos from the same clutch suggests that *her15* expression, like the other cyclic *her* genes, is dynamic before somitogenesis begins (Gajewski et al., 2003, 2006; Holley et al., 2000; Oates and Ho, 2002; Sieger et al., 2004; data not shown). At 80% epiboly, *her15* mRNA transcripts are detected in adaxial precursors (white arrow in Fig. 2B). Starting at the tail bud stage and continuing up to the 6-somite stage, variable *her15* mRNA expression in the posterior region of the PSM and tail bud was observed appearing in 3 distinguishable phases: “dot-like” –

with a small cluster of *her15*-expressing cells immediately posterior to the notochord (Fig. 2C); “intermediate” – a wave of expression appearing to move out radially from the dot-like domain (Figs. 2D, E); and finally “broad” – occupying almost the entire posterior of the PSM (Fig. 2F). During mid and late somitogenesis, dynamic *her15* expression in the posterior PSM persists (Figs. 2G–J). Lateral views of 12- to 16-somite stage embryos additionally reveal that the “dot-like” *her15* expression domain ranges through the tail bud from ventral to dorsal at the midline level (compare magnification of the tail bud region from Figs. 2I, J in K, L, respectively). Thus, *her15* is cyclically expressed in a unique manner in the tail bud restricted to the posterior PSM of zebrafish embryos.

To identify the phase relationship between *her15* and *her7* expression double *in situ* hybridisations were performed. These showed that in 10- to 12-somite stage wt embryos, the broad expression patterns of *her15* correlates with the elevated state of *her7* expression in the posterior PSM (Fig. 2M), whereas the dot-like expression patterns occur exclusively in conjunction with the reduced state of *her7* staining in this region (Fig. 2N). In the same assay, expression of *her12* mRNA was also found to be globally in phase with *her7* in the caudal PSM (Figs. 2O, P), consistent with the co-expression of *her12* and *her1* (Gajewski

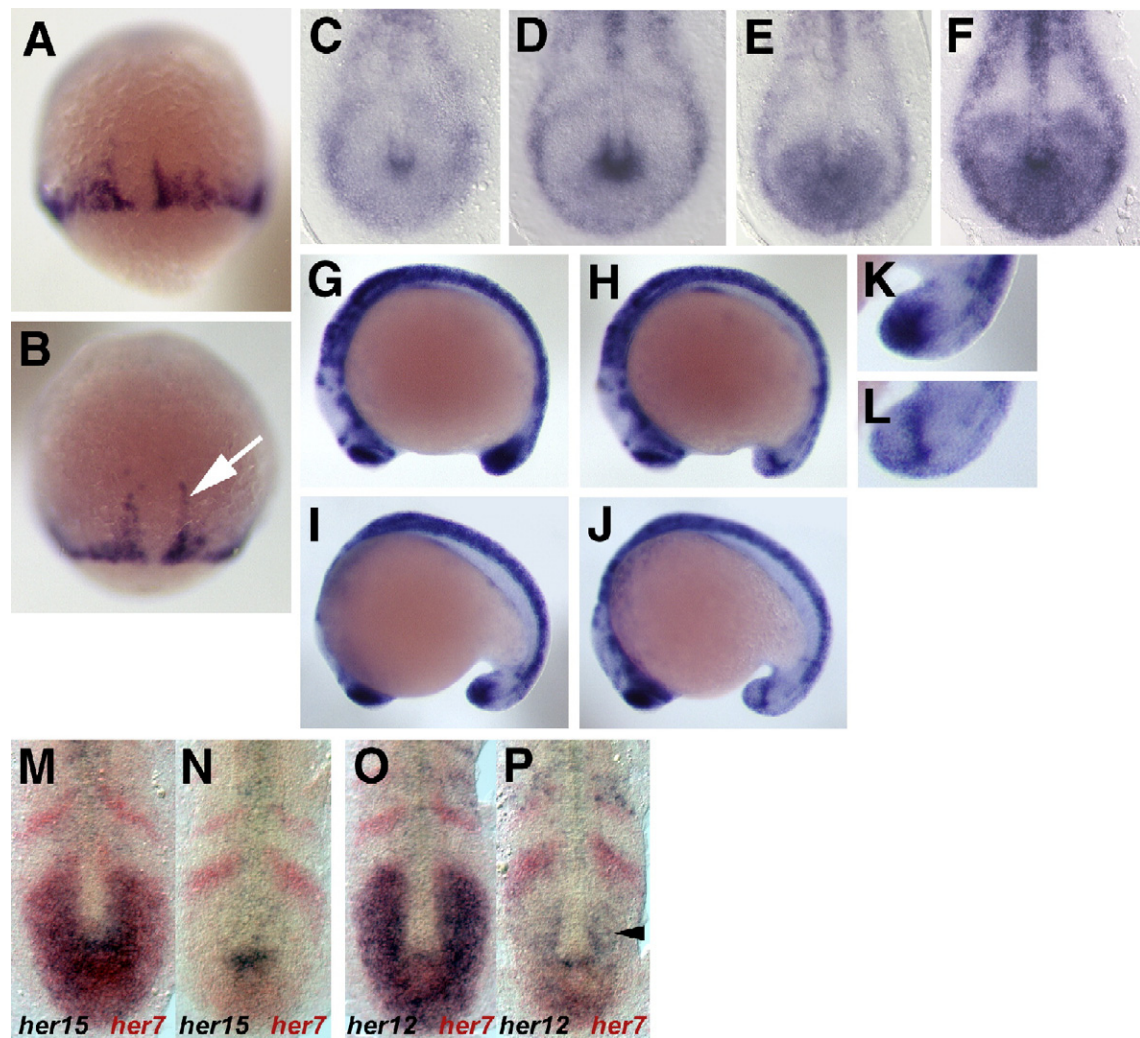


Fig. 2. Expression pattern analysis of *her15* in the caudal PSM. Expression of *her15* was analysed from 70% epiboly up to 16-somite stage focusing on the caudal PSM. Expression first appears during epiboly at the epibolic margin while the dorsal midline is devoid of transcript (A and B). Note expression on either side of the dorsal midline extends during epiboly towards the anterior pole (white arrow). At bud an expression domain is observed posterior to the notochord, which shows different width in a batch of embryos of nearly the same developmental stage (C–F). Due to narrowing and lengthening of the tail bud only broad and dot-like expression can unambiguously be distinguished in 12- to 14- (G and H, respectively) or 16- to 18-somite stage embryos (I and J, respectively; K and L are magnifications of the tail bud in panels I and J). During these stages it also becomes evident that the staining in the dot-like expression phase extends from ventral to dorsal in the midline of the tail bud (H and J). Wt embryos at the 10- to 12-somite stage were double-stained for *her7* transcripts (red) and *her15* (M, N) or *her12* (O, P) transcripts (blue). “Broad” staining patterns for *her15* and *her12* coincided with ubiquitous *her7* expression in the posterior PSM (M, O), “dot-like” *her15* and *her12* patterns were associated with low *her7* staining in this region (N, P). Arrowhead in panel P points to a region in the caudal PSM with *her12* transcription only, indicating slight phase shifts to *her7*.

et al., 2006). We conclude that the oscillations of both *her15* and *her12* are largely in phase with *her7* and therefore with *her1* as well (Oates and Ho, 2002; Gajewski et al., 2006). However, at certain time points in the cycle, cells in the anterior margin of the caudal co-oscillation domain show only *her12* expression (arrowhead), indicating that the *her7* and *her12* genes are not strictly co-expressed, consistent with a slight phase shift between the two.

The novel cyclic nature of the posterior expression domain was explored using the CLGY-521 enhancer trap line, in which an MMLV-*gata2*Promoter:YFP-containing retrovirus (Ellingsen et al., 2005) has inserted 535 bp 5' to the first exon of *her15b* on Chr 11 (Fig. 3A). This enhancer trap has been shown to work only when the basal *gata2*promoter:YFP-reporter is

integrated in the vicinity of an enhancer (Ellingsen et al., 2005). Under these circumstances, reporter gene expression in transgenic lines resembles expression of endogenous genes close to the insertion site. YFP protein could be detected throughout the paraxial mesoderm at 24 hpf in the CLGY-521 line (data not shown), due to the stability of the protein and consistent with our previous findings in *her1*promoter:GFP-reporter transgenic lines (Gajewski et al., 2003). In contrast, *in situ* hybridisation of the *yfp* transcript revealed a dynamic expression pattern restricted to the tail bud throughout segmentation stages. At bud stage, the levels of *yfp* expression in the tail bud could be divided into low and high classes (Figs. 3B, B'). At the 12-somite stage (Figs. 3C–E), expression consisted of a dorsal domain of cells with variable *yfp* levels

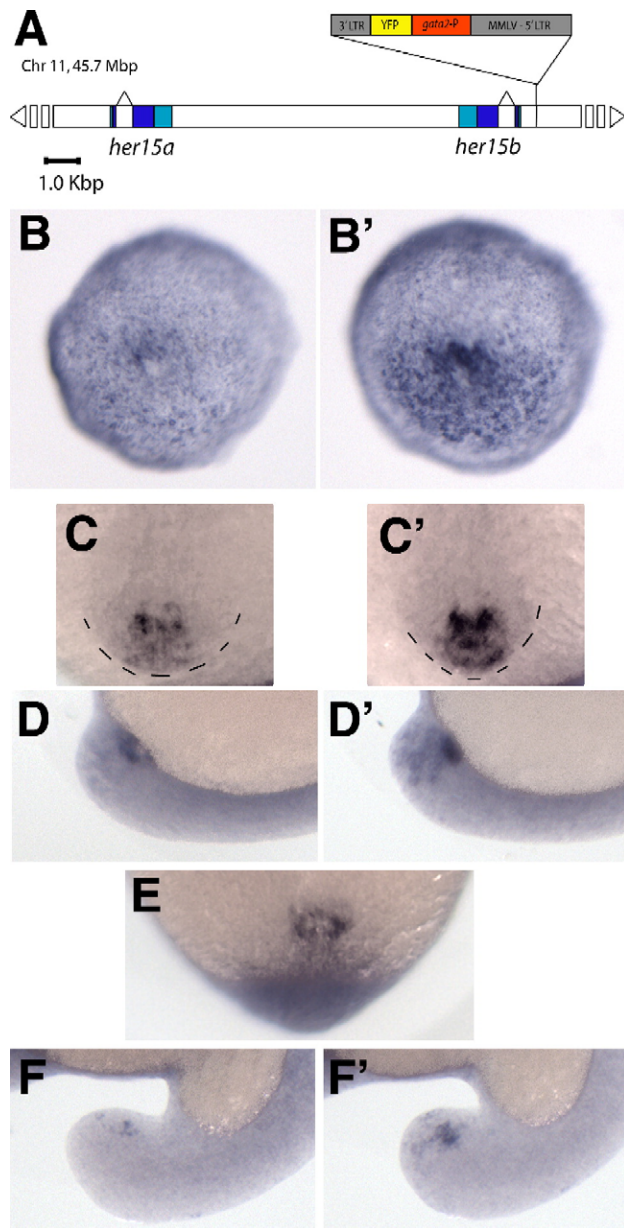


Fig. 3. Expression of the MMLV-retroviral enhancer trap CLGY-521 during somitogenesis. (A) Schematic representation of the CLGY-521 insertion site 535 bp 5' to the *her15b* gene on Chr 11, 45.7 Mbp. LTR=long terminal repeat, *gata2P*=zebrafish *gata2* promoter, YFP=yellow fluorescent protein. (B, B') Representative embryos from weak and strong expression classes, respectively, showing *yfp* mRNA distribution at bud stage; vegetal views, dorsal up. (C, C') Weak and strong expression classes at 12 somites, dorsal view of tail bud. (D, D') Same embryos in panels C, C' viewed laterally, to highlight the ventral core of expression. (E) Embryo from panels C, D viewed axially from posterior, to reveal the ring-like shape of expression domain. (F, F') Weak and strong expression classes at 17 somites, lateral view of tail bud.

(Figs. 3D, D') and a relatively constant ring-shaped ventral domain in the epithelium of Kupfer's vesicle (Fig. 3E). Variable tail bud expression was detected at the 17-somite stage (Figs. 3F, F'), but not at 26 hpf, when somitogenesis is finished (data not shown). We conclude that the expression pattern of the retroviral enhancer-trap closely mimics the highly variable posterior expression domain of *her15* gene at early stages (bud;

compare the wt expression in Figs. 2C–F with *yfp* expression in Figs. 3B and B'). We thus suggest that the transgene is under the control of a *her15b* enhancer that confers cyclic transcriptional activation in the posterior PSM and hence confirms the cyclic mode of at least the *her15b* gene duplicate. However, at later stages, *yfp*-expression, although dynamic, does not fully mimic endogenous *her15* oscillation anymore. Instead, *yfp*-expression is more restricted and the endogenous striped expression in the rostral PSM is not mirrored by the CLGY-521 line at all. This might indicate that further enhancers are necessary during the later somitogenesis period, which might not be detected by the integration close to the first *her15b* exon. Alternatively, the anterior expression domains may be a result of transcription from the *her15a* gene.

Expression and genetic regulation of her15, her12 and her4.1 in the rostral PSM

Around the 6- to 8-somite stage, one or two faint transverse stripes of *her15* expression first appeared in the rostral PSM, becoming stronger by the 8- to 12-somite stage (Figs. 4A–C). These *her15* mRNA expressing cells were detected in a limited number of sibling embryos (50–70%) from staged clutches, indicating that the RNA has a rapid turnover. Double *in situ* hybridisation with *myoD* was performed to determine the *her15* stripe positions in the rostral PSM. *myoD* is expressed in the posterior part of the already formed somites as well as in 2 stripes in the PSM. These two stripes mark the posterior compartment of the next two somites to be formed i.e. S0 and S-1 (Pourquié and Tam, 2001; Weinberg et al., 1996). The anterior-most *her15* stripe always prefigures or demarcates the border between S1 and S0 (Fig. 4F, black arrowhead), whereas the second stripe of *her15* expression, if present, is coincident with the most posterior *myoD* stripe in the PSM (Fig. 4F, white arrowhead) and thus this stripe is located at a two-segment distance from the more anterior stripe. The distance between the *her15* stripes was independently measured using as reference the width of the somite anterior to the first *her15* stripe (S2), which had two clearly visible somite borders. This measurement confirmed a two-segment interval between the *her15* expression stripes, whereas the anterior-most *her15* stripe occurs at a single-segment distance to the posterior border of the reference somite (ratio of interstripe distance to somite width=1.922; ratio of first stripe distance to reference somite=0.975; see Supplementary Table 1). We note that in rare cases (~4%), a third stripe of expression was detected between the two outer stripes (Fig. 4A).

Similar expression in thin stripes in the rostral PSM has been reported for *her4.1* and *her12* (Gajewski et al., 2006; Takke et al., 1999). Measurement of the distance between distinct *her4.1* stripes revealed a one-segment interval (Fig. 4L, Supplementary Table 1; ratio of first stripe distance to reference somite=0.933; ratio of interstripe distance to reference somite=1.044). Since the anterior *her4.1* stripe demarcates the last forming somite border as the anterior *her15* stripe (arrowhead, Fig. 4L, summarized in Fig. 4O), co-expression of *her4.1* with *her15* seems highly likely, but it is still not clear whether both stripes

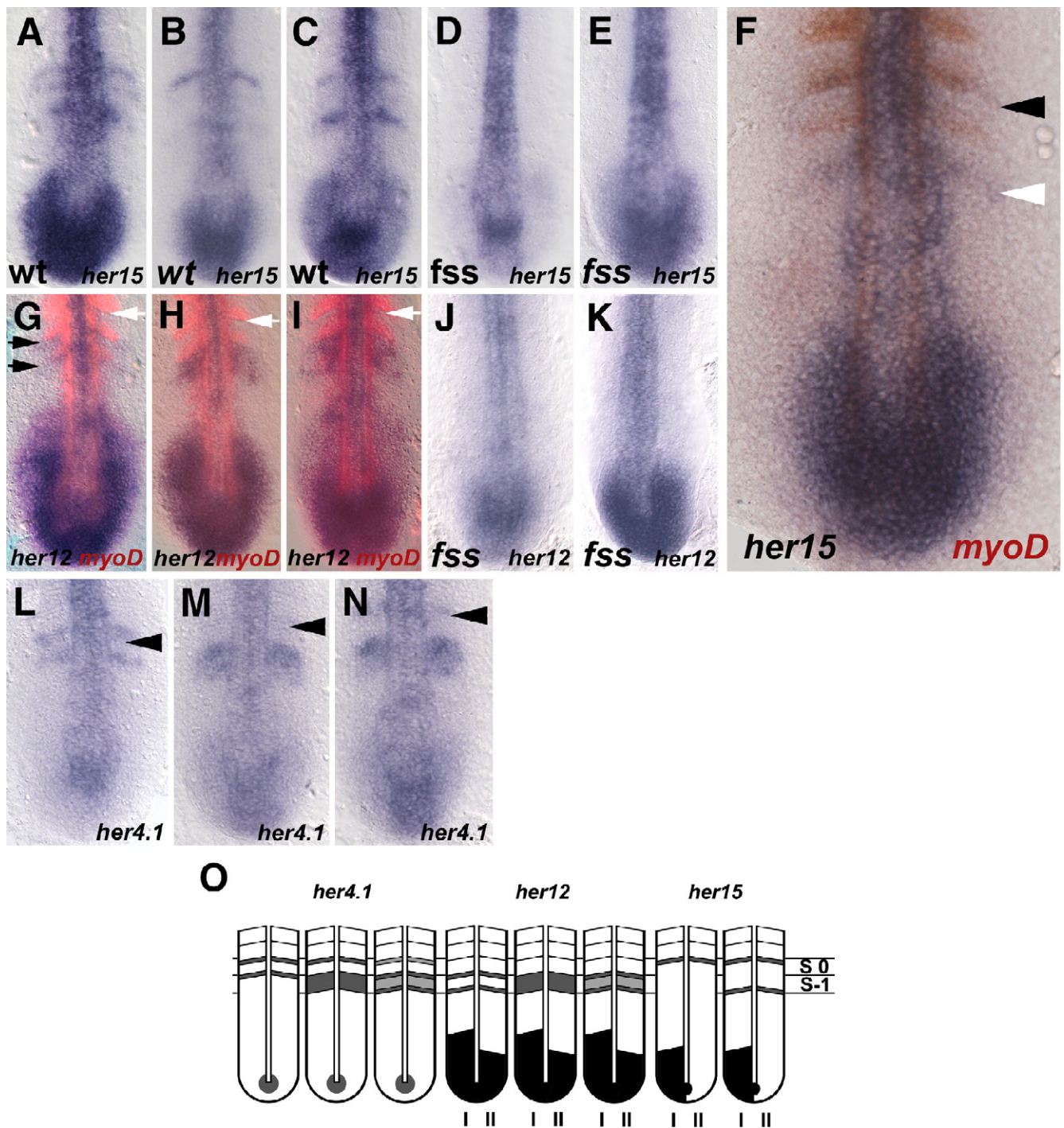


Fig. 4. Expression pattern analysis of the mHes5 homologues in the rostral PSM. (A–C, F) wt expression pattern of *her15*. At 8- to 10-somite stage *her15* expression was observed in one to two thin stripes in the rostral half PSM (A–C). These stripes occur in a double segmental distance at the future posterior somite borders of S1 and S-1, or when compared to *myoD* are co-expressed with the last *myoD* stripe and the *myoD* stripe within the last forming or formed somite (F). (D, E) *her15* expression in *fss*. (G–I) wt expression pattern of *her12* (blue) double-stained with *myoD* (red). (J, K) *her12* expression in *fss*. (L–N) wt expression pattern of *her4.1*. In contrast to *her15*, the stripes of *her12* and *her4.1* expression occur in a single segmental distance in the rostral PSM (G–I and L–N, respectively). (F) wt expression of *her15* (in blue) compared to *myoD* (in red). Black arrowhead points to the anterior-most *her15* and *her4* expression stripe, respectively, at the forming segment border. White arrowhead marks the posterior *her15* stripe, which is located in the last *myoD* stripe. Black arrow indicates the position of the two *her12* stripes matching with the penultimate and ultimate *myoD* stripe, respectively. White arrow marks the last formed segment border. (O) Schematic representation of the expression stripes of the mHes5 homologues in the rostral PSM. Location of the striped expression in the rostral PSM is compared between *her4.1*, *her12* and *her15*. Note, cyclic expression in the posterior is indicated by roman numbers I and II below the respective drawing. S0=somite, which will be formed next; S-1=prospective future somite posterior to S0.

are co-expressed throughout a complete expression period. The posterior *her4.1* expression stripe was variable, and could also be detected as a broader, one somite wide domain (Fig. 4M), which splits at the anterior and posterior border into two stripes in some embryos (Fig. 4N).

The position of *her12* stripes in the rostral PSM was also examined by double *in situ* hybridisation with *myoD*. In embryos with 2 stripes of *her12* expression, each lay immediately posterior to one of the last two *myoD* stripes in the PSM (Fig. 4G), whereas if only one broad *her12* stripe was detected, it was immediately posterior to the penultimate *myoD* stripe in the PSM (Fig. 4H). Embryos were also found with a broad *her12* stripe apparently splitting into two single stripes, located in between the posterior-most two *myoD* stripes (Fig. 4I). Taking the last formed somite border as a reference, we conclude that the next three prospective borders are marked by either *her4.1* together with *her15*, by *her4.1* and *her12*, or by all three *her* genes, respectively (see summary in Fig. 4O).

The fused somite (*fss*) mutant in zebrafish is characterized by the total absence of epithelial somite borders during the first 26 h of embryonic development and codes for the T-box gene *tbx24* (Nikaido et al., 2002). Although cyclic gene expression in the posterior PSM remains unaffected, *fss/tbx24* mutants fail to generate the narrowing stripes of *her1*, *her7* and *her11* in the intermediate to rostral PSM (van Eeden et al., 1998; Holley et al., 2002; Sieger et al., 2003, 2004). To investigate whether the *her12* and *her15* stripe regulation is likewise dependent on Tbx24, *her12* and *her15* expression patterns were analyzed in *fss/tbx24* mutants. As expected, the regionally oscillating expression in the posterior PSM was unaffected, whereas striped expression in the intermediate to anterior PSM was no longer observed (Figs. 4D, E for *her15* and Figs. 4J, K for *her12*). Hence, *her12* and *her15* stripe generation in the rostral PSM is dependent on Tbx24.

her12 and *her15* expression is differentially regulated by the Delta–Notch pathway

The *hE(spl)* genes play prominent roles in both neurogenesis and somitogenesis and, except for the *mHes6* homologues, are known targets of the Notch signaling pathway (Koyano-Nakagawa et al., 2000; Kawamura et al., 2005; Gajewski et al., 2006; Sieger et al., 2006). In particular, somitogenesis in zebrafish is regulated by the activity of *deltaC* (*dlc*) and *deltaD* (*dld*), via *notch1a* (*n1a*) and *Su(H)* signal transduction, on *her1*, *her7*, *her4*, *her6* and *her11* target genes in the PSM (Takke and Campos-Ortega, 1999; Holley et al., 2000, 2002; Henry et al., 2002; Oates and Ho, 2002; Gajewski et al., 2003; Pasini et al., 2004; Sieger et al., 2003, 2004; Oates et al., 2005). To investigate whether *her12* and *her15* are similarly regulated, their mRNA expression patterns were analyzed after inhibition of Notch signaling by DAPT treatment (Geling et al., 2002) or in *Su(H)* morphants (Sieger et al., 2003). The cyclic expression patterns of *her12* and *her15* were completely disrupted by DAPT and *Su(H)* morpholino treatments, leaving a diffuse, low-level staining in the posterior PSM. Further, the rostral PSM stripes were absent and down-regulation of expression

was observed in the posterior CNS (Figs. 5A–C for *her12* and Figs. 5H–J for *her15* expression in wt, *Su(H)* morphant and after DAPT treatment, respectively). In contrast, DAPT treatment only leads to disruption of *her1* and *her7* oscillation, but not to loss of expression in the rostral PSM (Horikawa et al., 2006; M.-C. Pauly and M. Gajewski, unpublished data). Thus, cyclic and rostral PSM expression of *her12* and *her15* is strictly dependent on Notch signaling.

To examine the contribution of individual *delta* or *notch* genes to the PSM, we analyzed expression patterns of *her12* and *her15* in the somitogenesis mutants *after eight* (*aei/dld*; Holley et al., 2000), *beamter* (*bea/dlc*; Julich et al., 2005), and *deadly seven* (*des/n1a*; Holley et al., 2002). In contrast to the effects of DAPT or *Su(H)* morpholinos, the posterior neural expression of *her12* and *her15* seem largely unaffected in the Delta–Notch mutants (Figs. 5D–F for *her12* and Figs. 5K–M for *her15* expression in *aei*, *bea* and *des*, respectively), which is likely due to the function of other *delta* and *notch* genes present in the zebrafish (Haddon et al., 1998; Westin and Lardelli, 1997).

Cyclic expression of *her15* in the posterior PSM and the striped expression in the rostral half of the PSM was strongly down-regulated at the 10- to 12-somite stage (Figs. 5K–M for *her15* expression in *aei*, *bea* and *des*), leaving a residual dot-like expression domain in the tail bud of all mutants. However, the presence of the posterior neuronal expression domain partly obscures the effects on cyclic expression when looking in dorsal view. Lateral views showed that *her15* transcripts in the ventral part of the residual expression domain were missing in *aei/dld*, but not in *bea/dlc* or *des/n1a* (compare Fig. 5O *her15* expression in *aei* with P–R, *her15* expression in *bea*, *des* and *Su(H)* morphant, respectively), suggesting that *deltaD* is necessary for *her15* expression in this region, whereas *deltaC* is needed for maintenance of *her15* oscillation throughout the tail bud. In contrast, both *deltaC* and *deltaD* are required for rostral PSM stripe formation. Cyclic posterior expression is already disturbed in *aei*, *bea*, *des* and *Su(H)* morphants at bud stage (Figs. 5S–V). Thus, all components of the Delta–Notch pathway examined are required for the regionally restricted, oscillating mRNA expression of the *her15* gene pair from bud throughout the somite formation period.

Cyclic *her12* expression in the PSM was clearly disrupted in all Delta–Notch mutants at 10–12 somites (Figs. 5D–F, *her12* expression in *aei*, *bea* and *des*, respectively), but as with *her15*, subtle differences were noted for each *delta* mutant. Expression in the posterior PSM was nearly absent in *aei/dld*, but a diffuse expression for *her12* could still be detected in the rostral PSM (Fig. 5D). *deltaC* seems to play a reciprocal role, since in *bea/dlc* embryos, *her12* expression was completely lost in the rostral PSM, but a weak staining was detected in the posterior (Fig. 5E). In *des/notch1a* mutants, *her12* expression was absent from the entire PSM, suggesting that both Delta signals are transmitted via Notch1a to activate *her12* (Fig. 5F). Thus, we conclude that the Notch pathway is required for the regulation of *her12* and *her15*, although different components contribute differentially to the posterior oscillation, the dorsal/ventral

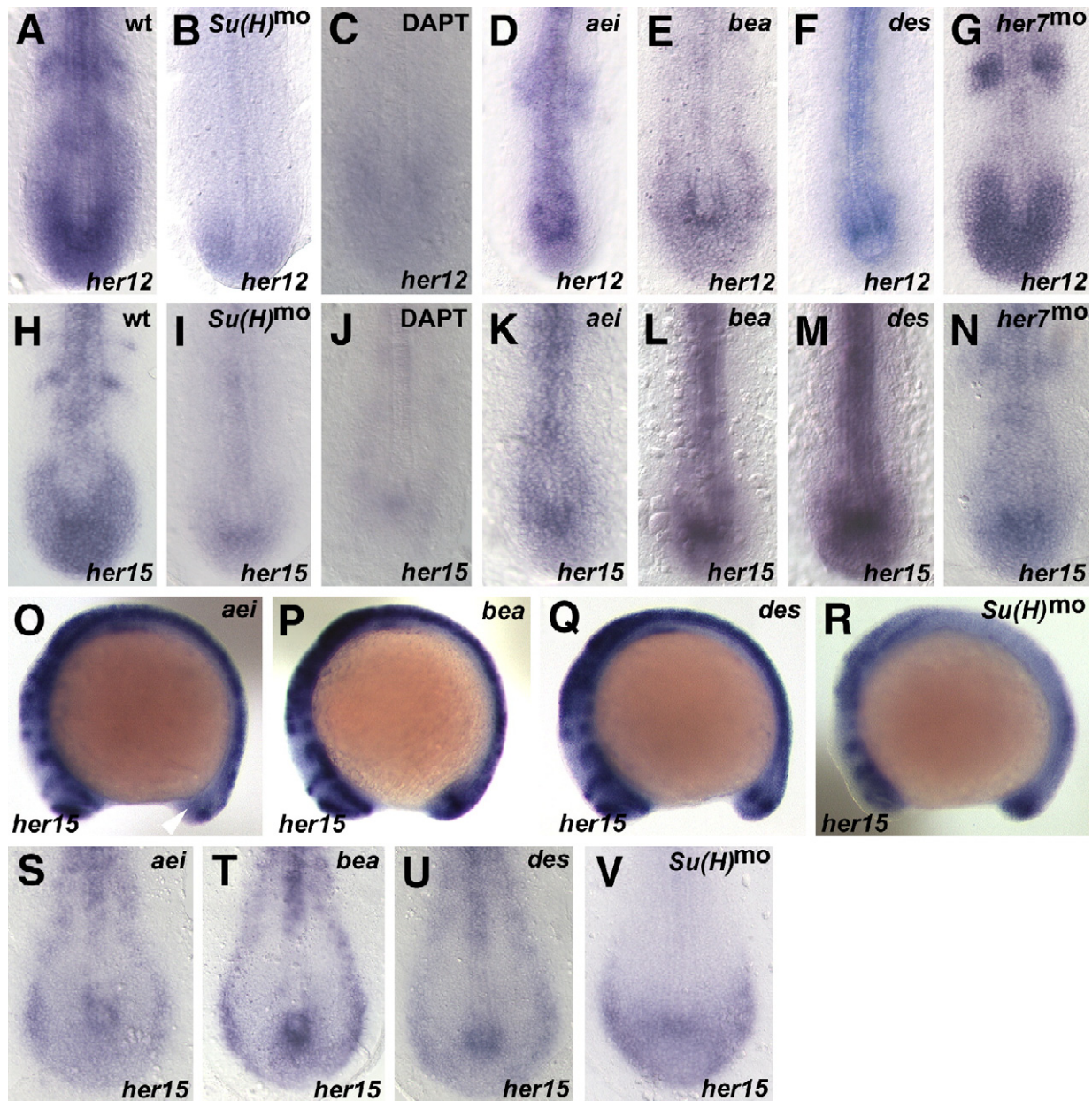


Fig. 5. Delta–Notch control of *her12* and *her15* expression. *her12* expression was examined in *Su(H)* morphants (2 experiments, $n=125$, 96% affected), after DAPT treatment (2 experiments, $n=41$, 98% affected), in the *fused somite* type mutants *aei/deltaD*, *bea/deltaC*, *des/notch1a* and in *her7* morphants (2 experiments, $n=93$, 85% affected) and compared to the respective wild type expression. Similarly, *her15* expression was analysed in *Su(H)* morphants (3 experiments, $n=21$, 100% affected), after DAPT treatment (2 experiments, $n=37$, 98% affected), in the *fused somite* type mutants *aei/deltaD*, *bea/deltaC*, *des/notch1a* and in *her7* morphants (2 experiments, $n=74$, 69% affected) and compared to the respective wild type expression. Wild type (wt) expression of *her12* and *her15* (A and H, respectively). Expression of *her12* and *her15* in *Su(H)* morphants (B and I), after DAPT treatment (C and J), in *aei* (D and K) in *bea* (E and L) and in *des* (F and M, respectively) at the 10- to 12-somite stage. (G and N) *her12* and *her15* expression in *her7* morphants, respectively. (O–R) (S–V) *her15* expression in *aei*, *bea*, *des* and *Su(H)* morphants at the 12- to 14-somite stage (in lateral view) and at bud stage, respectively. White arrowhead points to the ventral expression domain of *her15* that is only lost in the *aei* mutant situation.

aspects in the tail bud, and regulation of striped mRNA expression in the rostral PSM.

her12 and *her15* expression is regulated by *Her7*, but independent of *Her1*

The Notch target genes *her1* and *her7* are required for proper functioning of the segmentation clock (Gajewski et al.,

2003; Holley et al., 2002; Henry et al., 2002; Oates and Ho, 2002). *her1* and *her7* are largely co-expressed in the PSM, suggestive of a redundant function. Accordingly, morpholino knockdown of both genes in zebrafish embryos causes severe disruption of somite border formation and complete loss of cyclic expression patterns, whereas somite border formation is much weakly affected than oscillatory mRNA expression when knocking down *her1* or *her7* individually. To examine whether

her12 or *her15* are regulated by Her1 or Her7, their expression was analyzed in *her1* and *her7* morphants.

Interestingly, neither *her12* nor *her15* expression appeared affected in the PSM of *her1* morphants at the 10- to 12-somite stage (data not shown). In contrast, oscillatory *her15* expression was lost in *her7* morphants and only an intermediate level of *her15* mRNA expression was observed remaining in the tail bud (Fig. 5N). Only one stripe appeared in the rostral PSM, which was much broader and more penetrant than in wild type (Fig. 5H and Figs. 4A–C and F). Likewise, the posterior *her12* expression domain also showed intermediate expression levels without any signs of different cyclic phases and the rostral striped expression was disrupted in the *her7* knockdown embryos (compare Fig. 5G with Fig. 5A, Figs. 4G–I and Fig. 6 in Gajewski et al., 2006). These results indicate that Her7 is needed for maintenance of oscillating expression, and required for proper stripe formation of both *her12* and *her15*, while their expression appears independent of Her1 function.

Morpholino knockdown of *her12* perturbs cyclic expression but not somitogenesis

To test to what extent *her12* function is non-redundantly required during somitogenesis, we undertook a morpholino knock-down approach. Two specific morpholinos were designed, one against the start AUG of the *her12* ORF (ORF-Mo), and a mismatch Mo as control. Injection of the control Mo had no influence on somite morphology or cyclic gene expression. Injections of the *her12* ORF-Mo led to an obvious disruption of the expression of the cyclic genes *her1*, *her7* and *deltaC* at the 10- to 12-somite stage in approximately 50% of embryos (Figs. 6B, D, F), although no defects in somite border formation could be detected in the trunk. The relatively low

penetrance of cyclic expression defects compared to other knockdown approaches (Gajewski et al., 2003; Sieger et al., 2003) prompted the examination of *her12* ORF-Mo targeting efficiency. By using a fluorescent reporter mRNA containing the Mo-binding site, it could be revealed that the *her12* ORF-Mo exhibited a lower efficiency of 76% embryos showing reduction or absence of fluorescence than with other morpholinos obtained in the same assay, which show almost complete loss of fluorescence (Supplementary Fig. 1; Oates and Ho, 2002; Sieger et al., 2006). Higher concentrations of the *her12* morpholino caused pronounced shortenings of the embryos indicating non-specific, most probably toxic effects (Heasman, 2002, data not shown). Since *her12* ORF-morphants injected with 0.8 mM Mo were also often slightly shortened compared to control Mo-injected embryos, we assayed whether disruption of an early function of *her12* in the gastrula margin, potentially leading to improperly specified paraxial mesoderm, might lie upstream of the cyclic expression defects. The expression of *spt/tbx16*, a marker for paraxial mesoderm specification in the anterior trunk (Amacher et al., 2002; Griffin and Kimelman, 2002) was examined, but no difference could be detected between control and *her12* ORF-Mo injected embryos (Figs. 6G–J). This result implies that *her12* is not involved in specifying the paraxial mesoderm, but directly in the control of cyclic gene expression in the PSM.

her12 and *her15* over-expression disturbs the somitogenesis clock

Over-expression of *her1* mRNA in the zebrafish dramatically disrupts cyclic gene expression and somitogenesis (Takke and Campos-Ortega, 1999), indicating that the Her1 protein can interact with and disrupt the biochemistry of the segmentation

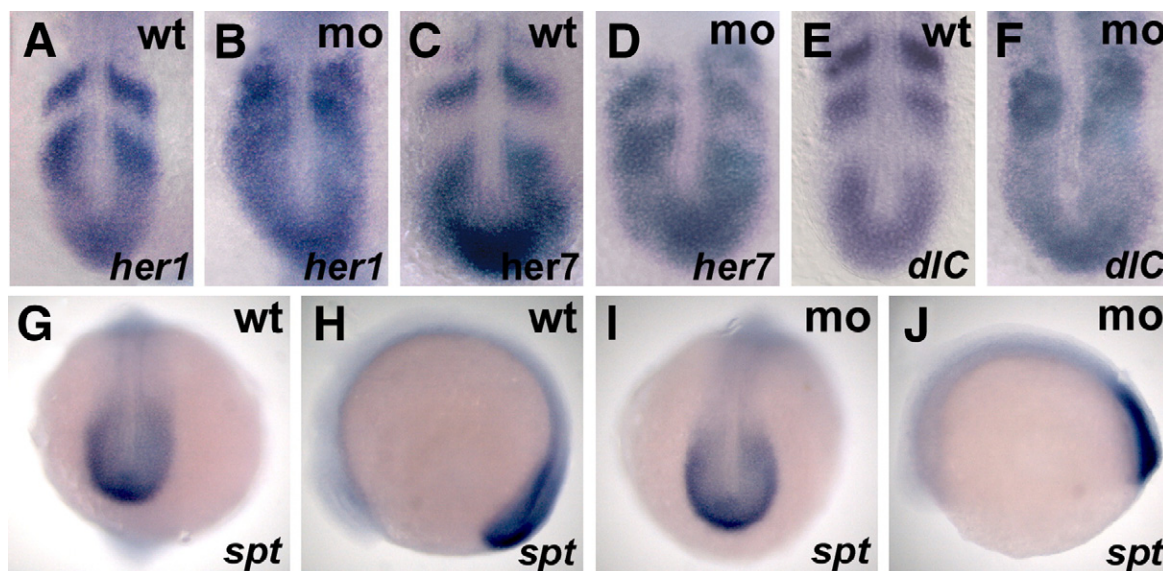


Fig. 6. Influence of the *her12*-ORF-Mo on gene expression in the PSM. (A, C, E) Wild type expression of *her1*, *her7* and *deltaC*, respectively. (B, D, F) Expression of *her1*, *her7* and *deltaC*, respectively, after *her12*-ORF-Mo injection (0.8 mM; 3 experiments for *her1*, $n=115$, 55% affected; 2 experiments for *her7*, $n=65$, 51% affected; 2 experiments for *deltaC*, $n=72$, 42% affected). (G, H) Wild type expression of *spt*, (I, J) *spt* expression in *her12* ORF-morphants (0.8 mM, 2 experiments, $n=68$, 96% of all embryos show wild type expression). (A–F) Flat-mounted embryos (8- to 10-somite stage), anterior to the top. (G–J) Whole mount embryos (10-somite stage); (G, I) dorsal view, posterior downwards; (H, J) lateral view, anterior to the left.

clock. However, none of the other cyclic *h/E(spl)* genes in zebrafish have been tested for this activity. We therefore investigated whether over-expression of Her11, Her12, Her15 or Her7 would show similar potential by injecting in vitro-transcribed mRNA at the single-cell stage and analyzing the embryos during somitogenesis stages (Fig. 7 for *her12* and *her15* and Fig. 8 for *her7*). As a control, *GFP* mRNA was injected at the same or higher concentration, and the majority of these embryos (>95%) developed normally and did not show any changes in cyclic expression patterns (Figs. 7A–C). Expression of *her11* mRNA did not overtly perturb somitogenesis at the 10 somite stage, although expression of *myoD* was more diffuse than in wild type, and disrupted *her1* expression was observed in 20–40% of injected embryos (data not shown). In contrast, injection of *her12* mRNA caused a disruption of somitic borders with high penetrance along the whole axis of the embryo, and slightly larger heads (Figs. 7D, E). Closer examination revealed that most of the somite borders were absent (Figs. 7C, F). In addition, embryos over-expressing *her12* show severe perturbations to the cyclic expression patterns of *her1*, *her7* and *deltaC*, indicating that the Her12 protein can interact with and perturb the clock mechanism (Figs. 7H, J and L).

Over-expression of *her15* mRNA led to somitogenic defects that were not restricted along the A/P axis, but of a lesser severity and penetrance than observed with *her12* mRNA (Figs. 7N, P). Cyclic expression of *deltaC*, *her1* (Figs. 7S, V) and *her7* (2 independent experiments, $n=28$, 54% embryos affected, data not shown) was also disrupted. Injection of higher concentrations of *her15* mRNA led to grossly abnormal embryos that could not be assayed for somite defects (data not shown), so no direct comparison of the relative activity of the *her15* and *her12* mRNAs should be inferred. These results indicate that the Her15 protein can also interact with and perturb the clock mechanism.

Over-expression of *her7* disturbs the segmentation clock

We, and others have previously shown that *her7* is required for normal segmentation, somitogenesis and cyclic gene expression (Oates and Ho, 2002; Gajewski et al., 2003; Henry et al., 2002), but the activity of Her7 protein has not yet been assayed. In *her7*-mRNA injected embryos, we observed disrupted expression of *myoD* in a concentration dependent manner (Figs. 8A, B; Table 1). Morphological somite defects co-localized with Myc-tagged Her7 protein (Fig. 8C), indicating that Her7 over-expression perturbs the process of somitogenesis. By pharyngula stages, due to muscle fiber elongation and the modification of the somite boundary into the transverse myoseptum, most somites have become distinctive chevron shaped myotomes that can be easily distinguished with a *titin* riboprobe (Oates and Ho, 2002; Fig. 8D). Embryos expressing *her7*, but not *lacZ* mRNA, displayed regions of segmental defects at 26 hpf that were distributed along the A/P axis without restriction (Figs. 8D, E; Table 1). These defects were of two basic types: a register defect with the loss of bilateral symmetry across the midline of otherwise normally shaped

myotomes; and boundary defect that was either bifurcated, partial or twisted in shape (arrow and arrowheads in Fig. 8E).

To determine whether the Her7-induced segmental defects might be due to a perturbation in the segmentation clock, we injected *her7* mRNA coding for a Myc-tagged variant and assayed the expression of *deltaC* and *her1* together with the location of Myc-epitope-expressing cells (Figs. 8F–I). The cyclic expression pattern of both *deltaC* and *her1* was perturbed only in embryos with Myc-reactivity in the PSM and paraxial mesoderm. Thus we conclude that elevated levels of Her7 in the PSM interact with and perturb the segmentation clock and so lead to segmentation defects.

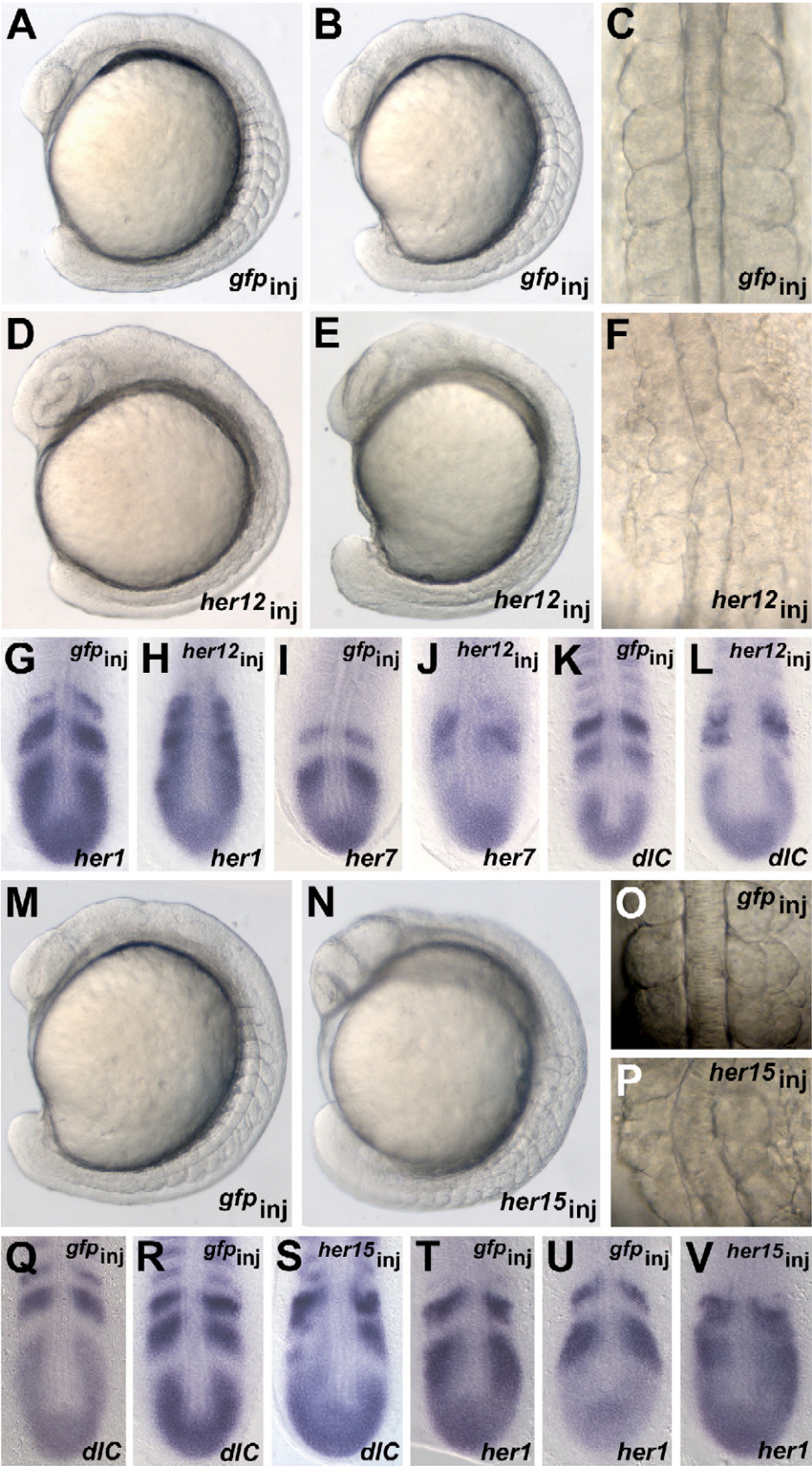
Activity of mutant *Her7* variants

In contrast to *her12* and *her15*, *her7* is an orthologue of the mouse cyclic *Hes7* gene (Sieger et al., 2004). *Hes7* has been shown to directly repress its own promoter and that of the *Lfng* gene (Bessho et al., 2003; Chen et al., 2005). To test whether regions of the Her7 protein predicted to mediate DNA binding and transcriptional repressor activities were required for perturbation of the segmentation clock, we used the generation of segmental abnormalities in 26 hpf embryos described above as an assay system for two mutant versions of Her7 mRNA (Table 1). Removal of the N-terminal domain responsible for DNA binding in the Her7 Δ bas construct reduced the incidence and severity of segmental defects, whereas removal of the C-terminal Groucho-interaction domain (Her7 Δ WRPW) did not (Table 1). These data suggest that at the mRNA concentrations examined, DNA binding plays a role in, but seems not essential for the segmentation defects, and that interaction with Groucho, or a Groucho-like cofactor may not be required.

Discussion

Distinct h/E(spl) cyclic expression domains sub-divide the tail bud and PSM

Since the initial discovery of *c-hairy1* mRNA oscillations in the chick PSM (Palmeirim et al., 1997), the number of known oscillating *h/E(spl)* family members has increased. Additional species, such as zebrafish, mouse and *Xenopus*, also possess cyclic *h/E(spl)* genes, and in each of these species multiple oscillating *h/E(spl)* genes have been identified (Dunwoodie et al., 2002; Jouve et al., 2000; Leimeister et al., 2000; Bessho et al., 2001a,b; Holley et al., 2000; Gajewski et al., 2003, 2006; Li et al., 2003; Oates and Ho, 2002; Sieger et al., 2004). We have now finished the genome-wide search for oscillating *h/E(spl)* genes in the near complete zebrafish sequence, and through the description of the *her15* gene pair in this paper, establish a total of five in this species. In contrast to amniote embryos, where the known *h/E(spl)* cyclic genes are co-expressed throughout the PSM and tail bud, we find that the cyclic *h/E(spl)* genes of zebrafish exhibit oscillatory expression in multiple distinct spatial configurations. Expression of *her1* and *her7* cycles in-phase throughout the PSM (Holley et al., 2000; Sawada et al., 2000; Oates and Ho, 2002; Henry et al., 2002; Gajewski et al.,



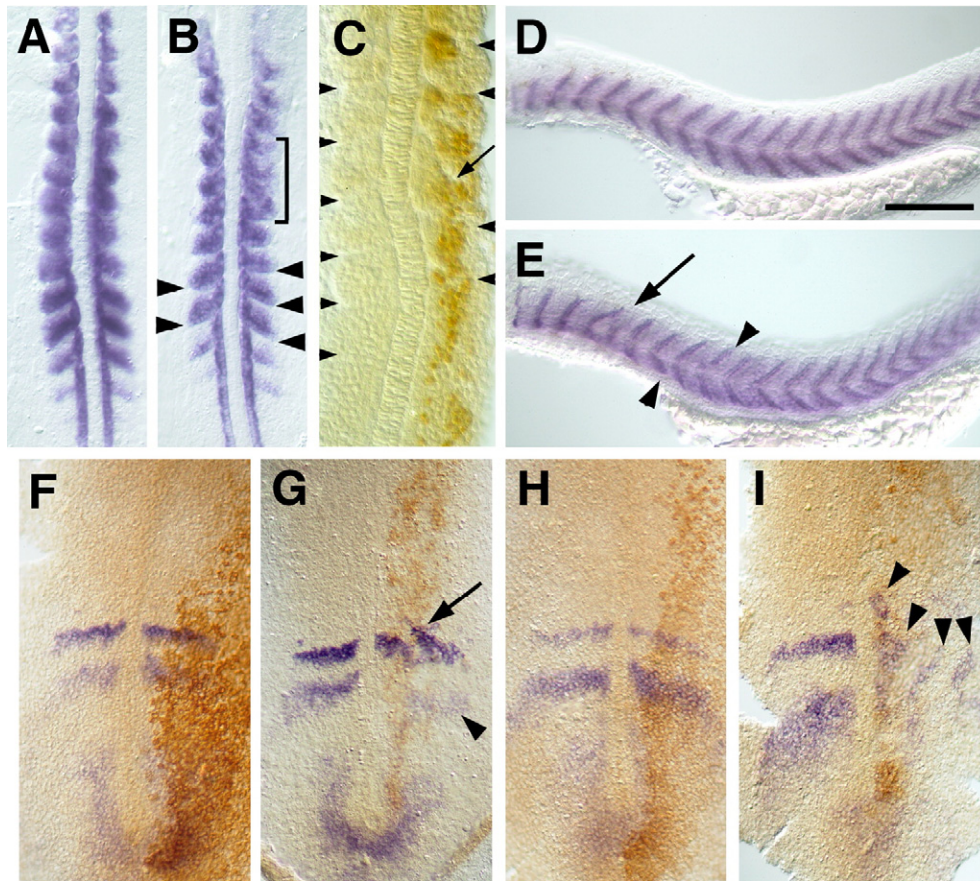






Fig. 8. Somitogenic and cyclic expression defects from *her7* mRNA over-expression. The expression of *myoD* in the presomitic mesoderm and trunk somites of embryos at 14 hpf (10 som, A, B) and cycling genes in the presomitic mesoderm at 10 hpf (1 som, F–I) are shown in dorsal view after flat mounting with anterior up. The myotome boundaries of the trunk marked by *titin* expression are shown in 26 hpf embryos in lateral view, anterior to the left and dorsal up (D, E). Scale bar in panel D is 250 μ m. Arrows and arrowheads indicate localized defects and brackets indicate the extent of larger regions of abnormalities. Expression of *myoD* after injection of *lacZ* (A) or *her7* mRNA (B). Segmentation defects of the trunk coincide with the region in which the Myc-tagged Her7 protein can be detected (C). Segmentation of the trunk after injection with *lacZ* mRNA (D) or *her7* mRNA (E). Expression of *delC* (F, G) and *her1* (H, I) after the injection of *gfp* (F, H) or *Myc-her7* mRNA (G, I).

2003), whereas *her11* expression oscillates only in the rostral half of the PSM in-phase with *her1* and *her7* (Sieger et al., 2004). The *her11* expression pattern is matched by a transgene containing a sub-fragment of the *her1* genomic regulatory region, suggesting that the rostral PSM expression domain may be controlled by a distinct enhancer element (Gajewski et al., 2003). A third domain is defined by the novel oscillating expression patterns of *her15* and *her12*, which both are restricted to the tail bud and caudal PSM. However, the cyclic expression domains of the *Hes5* paralogues are not identical, as the double stainings show (Fig. 2 and Gajewski et al., 2006).

From the perspective of a cell in the tail bud that is fated to enter the paraxial mesoderm and participate in somitogenesis, the configuration of oscillating *h/E(spl)* genes expressed will change with anterior displacement. Initially, *her12* and *her15* will be expressed together with *her1* and *her7*, but as the cell exits the tail bud, *her15* is down-regulated first, then *her12*, and finally *her11* is expressed to join the oscillatory process within the rostral PSM. In the rostral PSM *her4*, *her12* and *her15* each become expressed in a unique manner at the future somitic borders. In a posterior to anterior sequence, this occurs with all three at the posterior border of S-1, *her4* and *her12* at the

Fig. 7. Effects of *her12* and *her15* over-expression on somite morphology and clock genes. (A–C) *GFP*-RNA-injected embryos (850 ng/ μ l *GFP*-RNA, 2 experiments, $n=82$, 96% show wild type morphology). (D–F) *her12* RNA-injected embryos (800 ng/ μ l *her12*-RNA, 3 experiments, $n=102$, 44% affected). (G, I, K) *GFP*-RNA-injected embryos stained for *her1*, *her7* and *deltaC*, respectively (850 ng/ μ l *GFP*-RNA, 2 experiments, $n=96$, 95% show wild type expression). (H, J, L) *her12*-RNA-injected embryos stained for *her1*, *her7* and *deltaC*, respectively (800 ng/ μ l *her12*-RNA, 2 experiments, $n=104$, 48% affected). (M, O) *GFP*-RNA-injected embryos (150 ng/ μ l *GFP*-RNA, 4 experiments, $n=235$, 95% show wild type morphology). (N, P) *her15* RNA-injected embryos (115 ng/ μ l, 4 experiments, $n=219$, 44% show somite border defects). Note that another 34% of the injected embryos displayed gastrulation defects indicating that *her15* might act pleiotropically. In addition misexpression of *her15* caused severe brain defects resulting in improper brain patterning, enlarged brain vesicles and eye defects (compare M with N), while *her12* misexpression causes overall brain enlargement (compare A, B with D, E, respectively). Compared to *GFP*-mRNA control injections (Q, R and T, U, respectively) cyclic gene expression of *deltaC* (S) and *her1* (V) is disrupted. (A, B, D, E, M, N) whole mount embryos, lateral view, anterior to the upper left; (C, F, O, P) dorsal view, anterior to the top; (G–L and Q–V) flat-mounted embryos, anterior to the top; (A, C, D, F–L and Q–V) 10-somite stage embryos; (B, E and M–P) 14-somite stage embryos.

Table 1
Incidence and severity of segmental defects in zebrafish embryos over-expressing *her7* mRNA variants

Her7				
Her7Δbas				
Her7ΔWRPW				
Myc-Her7				
mRNA injected	pg per embryo	n	Somite disruption at 14 hpf ^a	Total segmental defects (%)
<i>her7</i>	240	8	4	50
	120	13	6	46
	60	17	7	41
	30	10	3	30
Segmental phenotype at 26 hpf ^b				
Normal Register Boundary Register and boundary				
Uninjected	0	38	38 (100)	0
<i>lacZ</i>	100	35	34 (97)	1 (3)
<i>her7</i>	100	35	13 (37)	4 (11)
<i>Myc-her7</i>	45	15	7 (47)	1 (7)
<i>her7Δbas</i>	45	9	8 (89)	0
<i>her7ΔWRPW</i>	100	20	14 (70)	1 (5)
	45	13	5 (38)	3 (23)
<i>her7ΔWRPW</i>	100	28	14 (50)	3
			3 (11)	8 (29)

^aSomite disruption was assessed with *myoD* expression at 14 hpf (10-somite stage).

^bSegmental phenotype was assayed by the shape of the transverse myoseptum at 26 hpf based on *titin in situ* hybridization. A register defect was the loss of bilateral symmetry across the midline of otherwise normally shaped myotomes. A boundary defect was the aberrant formation of a transverse myoseptum, either bifurcated, partial or twisted in shape.

posterior border of S0, and *her4* together with *her15* at the border forming between S1 and S0 (see Fig. 9 for a summary of the expression sequences of these *her* genes).

What consequence might this changing expression profile have for the function of the somitogenesis clock in the zebrafish? The ability of H/E(spl) proteins to dimerize led Leimeister et al. (2000) to propose the existence of a H/E(spl) bHLH “network” in the PSM, in which the formation of multiple homo- and heterodimers could provide redundancy, or diversity of action, in a combinatorial manner. In mouse and chick, the restricted expression of *Hey1* in nascent somites suggests that the activities of cyclic H/E(spl) proteins (which are otherwise all co-expressed across the posterior PSM and tail bud) could be modified by formation of heterodimers with *Hey1* only in the rostral-most PSM (Leimeister et al., 2000). Combined with our observations, we extend this idea, and propose that the Her-protein negative feedback loop, thought to be a central pacemaker of the somitogenesis clock (Guidicelli and Lewis, 2004), is not a single entity, but instead should be considered as a network that alters its composition along the A/P axis. Thus, current

models of oscillator function that utilize parameters derived from *her1* and *her7* are likely incomplete (Lewis, 2003), and inclusion of the outstanding *her* genes may be necessary to explain spatially dependent properties of oscillations in the PSM, such as their slowing and arrest. These changes could also account for other cell biological properties that change along the PSM, such as frequency of cell division, commitment to anterior and posterior somite fates, and cell-adhesion properties.

Rostral PSM expression of zebrafish *Hes5* homologues

A prominent feature of *Hes5* homologue expression in the zebrafish is the thin and dynamic stripes of expression in the rostral PSM that prefigure the forming morphological somite furrows. The position and timing of these stripes is consistent with a role in boundary formation or segment polarity. The high variability of *her15* stripe number between sibling embryos, and the existence of embryos without any rostral stripes strongly suggests that the expression associated with these domains is transient, generated by brief transcriptional pulses and producing unstable mRNA. The two-segment interval between rostral *her15* stripes seen in some embryos is a unique characteristic for a vertebrate gene, and is reminiscent of the *hairy* pair-rule gene in *Drosophila*, which is expressed in every alternate parasegment (Ish-Horowicz et al., 1985). It is tempting to once again suggest a link between the dipteran pair rule patterning mechanism and the vertebrate segmentation clock (Muller et al., 1996; Henry et al., 2002). But, alternatively, this double segmental expression feature could simply have been arisen secondarily by task splitting in the course of sub-functionalisation events in the duplicated *mHes5* homologues in zebrafish. In this light, the insertion of CLGY-521 into the potential upstream regulatory region of *her15b*, which lies distal to *her15a*, suggests a further sub-functionalisation event between the two most recent *her15* paralogues. CLGY-521 expression is a faith-

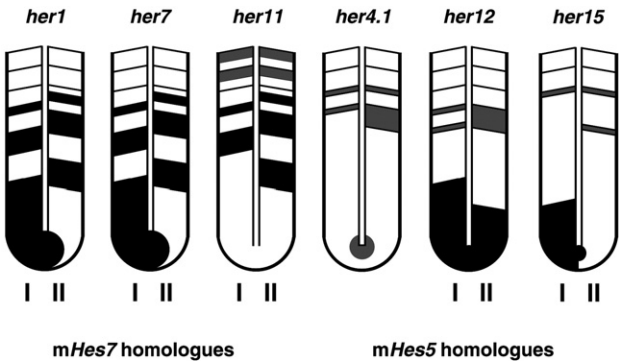


Fig. 9. Expression sequences of the *her* genes within the PSM. Schematic drawings of the dynamic expression modes of *her1*, *her7*, *her11* (the *mHes7* homologues) with *her4.1*, *her12* and *her15* (the *mHes5* homologues). The left and right halves indicate two different phases of the expression cycles, each, marked by (I) and (II) below the drawings, respectively. Expression patterns of *her1*, *her4.1*, *her7*, *her11* and *her12* are from Holley et al. (2000); Takke et al. (1999) and this study; Henry et al. (2002), Oates and Ho (2002) and Gajewski et al. (2003); Sieger et al. (2004); Gajewski et al. (2006) and this study, respectively.

ful copy of the posterior PSM expression pattern, but does not mimic the rostral stripes, or the neural domains (Fig. 3, data not shown). It is therefore possible that during the recent duplication event leading to *her15b*, an enhancer for the rostral stripes was left behind, leaving the newly formed gene copy only with posterior oscillatory regulation. Alternatively, CLGY-521 might be too far away from, or shielded from such a regulatory element that is still located 5' to *her15b*. In either case, the CLGY-521 line provides good support for the existence of a rostral stripe enhancer that is spatially distinct from the cyclic expression regulatory region.

In contrast to *her15*, *her4.1* and *her12* seem to be expressed initially in a stripe of one segment width at S-1, which later resolves into two stripes at a distance of a single segment during tail elongation. Again, embryos without any rostral *her12* stripe indicate that transcription is transient and thus dynamic (Gajewski et al., 2006), whereas *her4.1* expression seems to be more stable than *her12*, since additionally a stripe of expression was observed at the posterior border of S1, when a new stripe of segmental width is appearing caudal to this (see model in Fig. 4O). We conclude from our data, that the next three prospective borders are therefore marked in a unique code by the *mHes5* homologues.

her1, *her7* and *her11* expression domains also extend into the rostral PSM, but co-staining experiments reveal that these stripes are not stably co-expressed with those of *her12* and *her15* (Gajewski et al., 2006 and Figs. 2M–P). Although dynamic, *her12* and *her15* stripes rather seem to be expressed at a certain distance to the last formed somite and the *myoD* stripes (Figs. 4F and G–H), suggesting a different mechanism of regulation. Consistent with this, reduction of Notch signaling strongly reduces rostral *her12* and *her15* expression levels, whereas similar treatments affect the patterning, but not the levels of *her1*, *her7* and *her11* (Holley et al., 2000, 2002; Oates and Ho, 2002; Sieger et al., 2004). It is also possible that a complex cross-regulation between *her4.1*, *her12* and *her15* might occur in a similar manner to that seen between three *Hes5*-like genes during neurogenesis in chick (Fior and Henrique, 2005). Despite these differences in regulation by Delta/Notch signaling, all known *h/E(spl)* family genes in zebrafish require the T-box transcription factor Tbx24/fss for their rostral PSM expression (Holley et al., 2000; van Eeden et al., 1998; Sieger et al., 2003, 2004), suggesting conserved T-box regulatory elements. A loss of all *h/E(spl)* expression perhaps explains why the morphological somite phenotype of the *fss* mutant embryo is so severe, despite retaining cyclic expression in caudal domains (Holley et al., 2000; van Eeden et al., 1998; Sieger et al., 2003, 2004 and data presented in this study).

Delta–Notch signaling differentially regulates cyclic expression of the zebrafish Hes5 homologues

Despite the novel cyclic expression pattern of *her15* in the caudal region of the zebrafish embryo, the oscillations of both zebrafish *Hes5* homologues examined here appear to be controlled by Delta/Notch signaling, just as those of all other

known cyclic *h/E(spl)* family members. However, the observed spatio-temporal differences in PSM expression between the *mHes5* homologues in zebrafish do require a sophisticated and differential regulation regime. This has been shown in our study by detailed mutant and morphant analysis. The stripes and the posterior expression of *her12* appear to be differentially regulated via Delta–Notch signaling as it seems that DeltaD is necessary to initialise *her12* expression in the caudal PSM (absence of *her12* transcripts in *aei* in that region) whereas DeltaC is rather needed for the maintenance of the oscillation (expression is still there but oscillations are disrupted in *bea*). In the rostral PSM both ligands seem to have converse functions: DeltaD is needed for the maintenance of striped expression (*her12* transcripts are detectable, but striped expression is disturbed) whereas DeltaC is at least needed for stripe activation (Figs. 5D and E). Both ligands, in contrast, are involved in *her15* stripe regulation, at least for initialisation (absence of striped expression in both mutant situations) whereas Delta D is uniquely necessary to initialise *her15* oscillation in the posterior ventral subdomain and DeltaC is needed for the maintenance of the caudal cyclic expression (Figs. 5O and P; see Table 2 for a summary).

When the role of the different Delta ligands is compared with mouse, they play a conserved role on *mHes7*, *her1* and *her7*. With exception for *dll3* that is not involved in *mHes7* regulation at all, thus, *dll1*, *deltaC* and *deltaD* are necessary for maintenance of cyclic *mHes7*, *her1* and *her7* expression (see Table 2; Kusumi et al., 2004, and references therein). The role for both ligands (*dll1* and *dll3*) seems also to be similar for the mouse *Hes5* gene (Kusumi et al., 2004), because both are needed to activate *mHes5* transcription. In contrast, DeltaD and DeltaC play differential roles on the *mHes5* homologues *her12* and *her15* in zebrafish with respect to the caudal and rostral expression compartment (see Table 2 for a summary). Thus, the complexity of the process is uncovered by our analysis on the *mHes5* duplicates in zebrafish, which might be hidden in mouse.

The *her15* gene pair appears to have overlapping expression domains with *her4.1* in a small domain in the tail bud, at around the base of the notochord. This intriguing region may harbor tail stem cells, by analogy to the mouse (Nicolas et al., 1996), or it may host some persistent pace making activity as it has been suggested for chicken (Liu et al., 2004). Clearly, further experiments are required to understand the anatomy and function of the zebrafish tail bud (Kanki and Ho, 1997).

Table 2
Role of the different Delta ligands in mouse and zebrafish

Initiation		Maintenance	
Dll1 • <i>mHes7</i>	X	Dll1 • <i>mHes5</i>	X
ΔD • <i>her1</i>	X	ΔD • <i>her12</i>	X _c X _r
ΔD • <i>her7</i>	X	ΔD • <i>her15</i>	X _v X _r
Dll3 • <i>mHes7</i>	–	Dll3 • <i>mHes5</i>	X
ΔC • <i>her1</i>	X	ΔC • <i>her12</i>	X _r X _c
ΔC • <i>her7</i>	X	ΔC • <i>her15</i>	X _r X _c

Indices give the position within the PSM at which the respective ligand–target gene interaction was observed: c, caudal; r, rostral; v, ventral; data for the mouse genes are from Kusumi et al. (2004, and references therein).

A role for her12 and her15 in the somitogenesis clock

Disruption of cyclic expression patterns throughout the tail bud and PSM after *her12* Mo knockdown clearly indicates that *her12* is a critical component required for the control of gene oscillations in the PSM. However, in contrast to *her7* Mo knockdown (Oates and Ho, 2002; Gajewski et al., 2003), some striped expression remained within the disrupted cyclic pattern in some embryos. Since efficiency controls indicate that the *her12*-targeting morpholino does not fully block translation, we suspect that the incompletely penetrant phenotype we observed simply reflects the incomplete loss of protein activity. In previous *her7* knockdown experiments, which yielded posterior somite defects, we noted a window of time preceding the first somitic defects, in which cyclic expression was abnormal (Fig. 4 in Oates and Ho, 2002); this gradual decay of cyclic expression domains concomitant with apparently normal somite morphology has also been noted for Delta/Notch mutants or *Su(H)* morphants (Jiang et al., 2000; Oates et al., 2005; Sieger et al., 2003). Thus there is clear precedence for the ability of the segmentation clock to sustain somite formation when partially compromised. This robustness is likely the explanation for the lack of morphological effects on somite formation seen in our *her12* morphants, despite perturbation of cyclic expression.

Targeting *her15* with morpholinos resulted neither in a visible somitogenesis-related phenotype, nor in defects in cyclic expression patterns, although effects on brain morphology were observed (S.S. unpublished observation), suggesting that the *her15* Mo was at least partially functional. However, the existence of the recently duplicated *her15* gene pair with identical 5'UTR sequence may reduce the effectiveness of injected Mo, yielding only a hypomorphic situation at non-toxic concentrations of Mo. Double knock-down with *her12*, *her1*, *her7*, *her11* or *her13.2* morpholinos did not reveal a synergistic phenotype as was observed for *her1* and *her7* or *her1* and *her13.2* double morphants (Henry et al., 2002; Oates and Ho, 2002; Sieger et al., 2006, and data not shown) and attempts to test triple knock-down were frustrated by non-specific defects due to high Mo concentration (data not shown).

In genetic systems with high redundancy, loss of function studies can overlook components with important roles. These components may nevertheless be identified with gain of function approaches. For example, although an important, but redundant role for *her1* in the zebrafish segmentation clock has been identified through double knockdown with *her7*, *her11* or *her13.2* genes, *her1* single-gene knockdowns yield extremely weak phenotypes (Henry et al., 2002; Oates and Ho, 2002; Sieger et al., 2004, 2006). In contrast, over-expression of *her1* results in striking somite and cyclic expression defects (Takke and Campos-Ortega, 1999), revealing the potential of the Her1 protein to interact with and perturb the molecular mechanism of the somitogenesis clock. Importantly, detectable somitogenic defects have not been reported after over-expression of mRNA from *h/E(spl)* genes not endogenously expressed in the PSM such as *her3*, *her5* or *her9* (Geling et al., 2003; Hans et al., 2004; Latimer et al., 2005), and conversely, over-expression of *her1* mRNA does not perturb neural development (Takke et al.,

1999). In addition, the over-expression phenotypes described here are clearly different from the *her4/her6* misexpression results (this study; Pasini et al., 2004). All of these findings argue that the effects on somitogenesis caused by over-expression of *her7*, *her12* and *her15* mRNA are specific, and not general responses to an elevated level of H/E(spl) protein.

The functional analyses done in this study suggest that *her12* and *her15* are involved in both the regulation of cyclic gene expression and the formation of somite borders. Misexpression of *her12*, and albeit much weaker for *her15*, leads to disruption of core clock expression and somite formation. In addition, expression of *her12* and *her15* is controlled by all known zebrafish core clock elements as our mutant and morphant analyses have shown. Thus, we suggest that mHes5 homologues might be parts of the core clock, or at least strongly interfere with the control of the oscillation machinery, as has been shown for *her1* and *her7* (Gajewski et al., 2003; Henry et al., 2002; Holley et al., 2000; Oates and Ho, 2002), rather than simply being an output of the clock.

The ability of exogenous H/E(spl) proteins to perturb the segmentation clock could in principle arise from several features of their biochemistry. A sustained, increased level of the over-expressed homodimer could occupy elements in the promoters of target genes, thereby over-repressing them and, in the case of cyclic target genes, damping their oscillations. Alternatively, by forming heterodimers with the endogenous cyclic H/E(spl) proteins, or by titrating out non-cyclic binding partners such as Her13.2 (Kawamura et al., 2005), the proportion of specific heterodimeric subtypes may be altered, potentially causing a change in the repression and activation of multiple target genes. Our structure function analysis of Her7 suggests that DNA binding activity may be involved in the perturbation of the segmentation clock, but that the ability to bind members of the Groucho family of co-repressors might not. This Her7 structure/function relationship mimics that of the Her4 protein during neurogenesis (Takke et al., 1999), consistent with a common mode of action for H/E(spl) proteins independent of their subfamily or specific developmental process. Thus, a simple Groucho-dependent over-repression of targets by exogenous homodimeric Her7 in the PSM seems an unlikely mechanism. From our results we speculate that the formation of DNA-binding heterodimers between the over-expressed Her7, Her12 or Her15 proteins and other H/E(spl) proteins in the tail bud and PSM might alter the balance of dimeric species along the PSM, and it may be this effect that principally perturbs the segmentation clock. The consequence of this view, in which the balance of heterodimers are vital, is that the phenotype of a loss of function of a single cyclic *her* gene cannot be viewed simply as the removal of one molecular species. It should instead be regarded as the outcome of a cascade of alterations that affect the activity of multiple H/E(spl)-containing complexes in the tail bud and PSM.

Acknowledgments

The people from the Tautz lab would like to thank Diethard Tautz for his continuous support in the somitogenesis research

project. We thank Laurel Rohde for critical reading of the manuscript, Robert Ho, in whose laboratory some of the *her7* experiments were performed, and Mario Caccamo from the Sanger Centre, Cambridge for help with bioinformatics. We also wish to thank Irene Steinfartz, Eva Schetter and Claudia Müller for excellent technical assistance, the fish facility of the MPI-CBG and David and Carsten from the fish facility of the Institute for Genetics in Cologne. The work was supported by the Deutsche Forschungsgemeinschaft (SFB 572) and by the Fond der chemischen Industrie. S.S. was the first graduate of the “International Graduate School in Genetics and Functional Genomics” of the University of Cologne.

Appendix A. Supplementary data

Supplementary data associated with this article can be found, in the online version, at doi:10.1016/j.ydbio.2007.01.004.

References

- Amacher, S.L., Draper, B.W., Summers, B.R., Kimmel, C.B., 2002. The zebrafish T-box genes *no tail* and *spadetail* are required for development of trunk and tail mesoderm and medial floor plate. *Development* 129, 3311–3323.
- Bae, Y.K., Shimizu, T., Hibi, M., 2005. Patterning of proneuronal and interproneuronal domains by *hairy*- and *enhancer of split*-related genes in zebrafish neuroectoderm. *Development* 132, 1375–1385.
- Bessho, Y., Kageyama, R., 2003. Oscillations, clocks and segmentation. *Curr. Opin. Genet. Dev.* 13, 379–384.
- Bessho, Y., Miyoshi, G., Sakata, R., Kageyama, R., 2001a. *Hes7*: a bHLH-type repressor gene regulated by Notch and expressed in the presomitic mesoderm. *Genes Cells* 6, 175–185.
- Bessho, Y., Sakata, R., Komatsu, S., Shiota, K., Yamada, S., Kageyama, R., 2001b. Dynamic expression and essential functions of *Hes7* in somite segmentation. *Genes Dev.* 15, 2642–2647.
- Bessho, Y., Hirata, H., Masamizu, Y., Kageyama, R., 2003. Periodic repression by the bHLH factor *Hes7* is an essential mechanism for the somite segmentation clock. *Genes Dev.* 17, 1451–1456.
- Bruce, A.E., Oates, A.C., Prince, V.E., Ho, R.K., 2001. Additional *hox* clusters in the zebrafish: divergent expression patterns belie equivalent activities of duplicate *hoxB5* genes. *Evol. Dev.* 3, 127–144.
- Chen, J., Kang, L., Zhang, N., 2005. Negative feedback loop formed by Lunatic fringe and *Hes7* controls their oscillatory expression during somitogenesis. *Genesis* 43, 196–204.
- Davis, R.L., Turner, D.L., 2001. Vertebrate *hairy* and *Enhancer of split* related proteins: transcriptional repressors regulating cellular differentiation and embryonic patterning. *Oncogene* 20, 8342–8357.
- del Barco Barrantes, I.B., Elia, A.J., Wunsch, K., Hrabe de Angelis, M.H., Mak, T.W., Rossant, J., Conlon, R.A., Gossler, A., de la Pompa, J.L., 1999. Interaction between Notch signalling and Lunatic fringe during somite boundary formation in the mouse. *Curr. Biol.* 9, 470–480.
- Dunwoodie, S.L., Clements, M., Sparrow, D.B., Sa, X., Conlon, R.A., Beddington, R.S., 2002. Axial skeletal defects caused by mutation in the spondylocostal dysplasia/pudgy gene *Dil3* are associated with disruption of the segmentation clock within the presomitic mesoderm. *Development* 129, 1795–1806.
- Ellingsen, S., Laplante, M.A., Konig, M., Kikuta, H., Furmanek, T., Hoivik, E.A., Becker, T.S., 2005. Large-scale enhancer detection in the zebrafish genome. *Development* 132, 3799–3811.
- Fior, R., Henrique, D., 2005. A novel *hes5/hes6* circuitry of negative regulation controls Notch activity during neurogenesis. *Dev. Biol.* 281, 318–333.
- Gajewski, M., Voolstra, C., 2002. Comparative analysis of somitogenesis related genes of the *hairy/Enhancer of split* class in Fugu and zebrafish. *BMC Genomics* 3, 21.
- Gajewski, M., Sieger, D., Alt, B., Leve, C., Hans, S., Wolff, C., Rohr, K.B., Tautz, D., 2003. Anterior and posterior waves of cyclic *her1* gene expression are differentially regulated in the presomitic mesoderm of zebrafish. *Development* 130, 4269–4278.
- Gajewski, M., Elmasri, H., Girschick, M., Sieger, D., Winkler, C., 2006. Comparative analysis of *her* genes during fish somitogenesis suggests a mouse/chick-like mode of oscillation in medaka. *Dev. Genes Evol.* 216, 315–332.
- Geling, A., Steiner, H., Willem, M., Bally-Cuif, L., Haass, C., 2002. A gamma-secretase inhibitor blocks Notch signaling in vivo and causes a severe neurogenic phenotype in zebrafish. *EMBO Rep.* 3, 688–694.
- Geling, A., Itoh, M., Tallafuss, A., Chapouton, P., Tannhauser, B., Kuwada, J.Y., Chitnis, A.B., Bally-Cuif, L., 2003. bHLH transcription factor *Her5* links patterning to regional inhibition of neurogenesis at the midbrain–hindbrain boundary. *Development* 130, 1591–1604.
- Giudicelli, F., Lewis, J., 2004. The vertebrate segmentation clock. *Curr. Opin. Genet. Dev.* 14, 407–414.
- Griffin, K.J., Kimelman, D., 2002. One-eyed pinhead and spadetail are essential for heart and somite formation. *Nat. Cell Biol.* 4, 821–825.
- Haddon, C., Smithers, L., Schneider-Maunoury, S., Coche, T., Henrique, D., Lewis, J., 1998. Multiple *delta* genes and lateral inhibition in zebrafish primary neurogenesis. *Development* 125, 359–370.
- Hans, S., Scheer, N., Riedl, I., v Weizsacker, E., Blader, P., Campos-Ortega, J.A., 2004. *her3*, a zebrafish member of the *hairy-E(spl)* family, is repressed by Notch signalling. *Development* 131, 2957–2969.
- Heasman, J., 2002. Morpholino oligos: making sense of antisense? *Dev. Biol.* 243, 209–214.
- Henry, C.A., Urban, M.K., Dill, K.K., Merlie, J.P., Page, M.F., Kimmel, C.B., Amacher, S.L., 2002. Two linked *hairy/Enhancer of split*-related zebrafish genes, *her1* and *her7*, function together to refine alternating somite boundaries. *Development* 129, 3693–3704.
- Hirata, H., Bessho, Y., Kokubu, H., Masamizu, Y., Yamada, S., Lewis, J., Kageyama, R., 2004. Instability of *Hes7* protein is crucial for the somite segmentation clock. *Nat. Genet.* 36, 750–754.
- Holley, S.A., Geisler, R., Nusslein-Volhard, C., 2000. Control of *her1* expression during zebrafish somitogenesis by a delta-dependent oscillator and an independent wave-front activity. *Genes Dev.* 14, 1678–1690.
- Holley, S.A., Julich, D., Rauch, G.J., Geisler, R., Nusslein-Volhard, C., 2002. *her1* and the notch pathway function within the oscillator mechanism that regulates zebrafish somitogenesis. *Development* 129, 1175–1183.
- Horikawa, K., Ishimatsu, K., Yoshimoto, E., Kondo, S., Takeda, H., 2006. Noise-resistant and synchronized oscillation of the segmentation clock. *Nature* 441, 719–723.
- Huppert, S.S., Ilagan, M.X., De Strooper, B., Kopan, R., 2005. Analysis of Notch function in presomitic mesoderm suggests a gamma-secretase-independent role for presenilins in somite differentiation. *Dev. Cell* 8, 677–688.
- Ish-Horowicz, D., Howard, K.R., Pinchin, S.M., Ingham, P.W., 1985. Molecular and genetic analysis of the hairy locus in *Drosophila*. *Cold Spring Harbor Symp. Quant. Biol.* 50, 135–144.
- Ishibashi, M., Ang, S.L., Shiota, K., Nakanishi, S., Kageyama, R., Guillemot, F., 1995. Targeted disruption of mammalian *hairy* and *Enhancer of split* homolog-1 (*HES-1*) leads to up-regulation of neural helix–loop–helix factors, premature neurogenesis, and severe neural tube defects. *Genes Dev.* 9, 3136–3148.
- Jensen, J., Pedersen, E.E., Galante, P., Hald, J., Heller, R.S., Ishibashi, M., Kageyama, R., Guillemot, F., Serup, P., Madsen, O.D., 2000. Control of endodermal endocrine development by *Hes-1*. *Nat. Genet.* 24, 36–44.
- Jiang, Y.J., Aerne, B.L., Smithers, L., Haddon, C., Ish-Horowicz, D., Lewis, J., 2000. Notch signalling and the synchronization of the somite segmentation clock. *Nature* 408, 475–479.
- Jouve, C., Palmeirim, I., Henrique, D., Beckers, J., Gossler, A., Ish-Horowicz, D., Pourquie, O., 2000. Notch signalling is required for cyclic expression of the hairy-like gene *HES1* in the presomitic mesoderm. *Development* 127, 1421–1429.
- Julich, D., Hwee Lim, C., Round, J., Nicolaije, C., Schroeder, J., Davies, A., Geisler, R., Lewis, J., Jiang, Y.J., Holley, S.A., 2005. *beamter/deltaC* and the role of Notch ligands in the zebrafish somite segmentation,

- hindbrain neurogenesis and hypochord differentiation. *Dev. Biol.* 286, 391–404.
- Kanki, J.P., Ho, R.K., 1997. The development of the posterior body in zebrafish. *Development* 124, 881–893.
- Kawamura, A., Koshida, S., Hijikata, H., Sakaguchi, T., Kondoh, H., Takada, S., 2005. Zebrafish hairy/enhancer of split protein links FGF signaling to cyclic gene expression in the periodic segmentation of somites. *Genes Dev.* 19, 1156–1161.
- Koyano-Nakagawa, N., Kim, J., Anderson, D., Kintner, C., 2000. *Hes6* acts in a positive feedback loop with the neurogenins to promote neuronal differentiation. *Development* 127, 4203–4416.
- Kusumi, K., Mimoto, M.S., Covelio, K.L., Beddington, R.S., Krumlauf, R., Dunwoodie, S.L., 2004. *Dll3* pudgy mutation differentially disrupts dynamic expression of somite genes. *Genesis* 39, 115–121.
- Latimer, A.J., Shin, J., Appel, B., 2005. *her9* promotes floor plate development in zebrafish. *Dev. Dyn.* 232, 1098–1104.
- Leimeister, C., Dale, K., Fischer, A., Klamt, B., Hrabe de Angelis, M., Radtke, F., McGrew, M.J., Pourquie, O., Gessler, M., 2000. Oscillating expression of c-Hey2 in the presomitic mesoderm suggests that the segmentation clock may use combinatorial signaling through multiple interacting bHLH factors. *Dev. Biol.* 227, 91–103.
- Leve, C., Gajewski, M., Rohr, K.B., Tautz, D., 2001. Homologues of c-hairy1 (*her9*) and lunatic fringe in zebrafish are expressed in the developing central nervous system, but not in the presomitic mesoderm. *Dev. Genes Evol.* 211, 493–500.
- Lewis, J., 2003. Autoinhibition with transcriptional delay: a simple mechanism for the zebrafish somitogenesis oscillator. *Curr. Biol.* 13, 1398–1408.
- Li, Y., Fenger, U., Niehrs, C., Pollet, N., 2003. Cyclic expression of *esr9* gene in *Xenopus* presomitic mesoderm. *Differentiation* 71, 83–89.
- Liu, C., Knezevic, V., Mackem, S., 2004. Ventral tail bud mesenchyme is a signaling center for tail paraxial mesoderm induction. *Dev. Dyn.* 229, 600–606.
- Masamizu, Y., Ohtsuka, T., Takashima, Y., Nagahara, H., Takenaka, Y., Yoshikawa, K., Okamura, H., Kageyama, R., 2006. Real-time imaging of the somite segmentation clock: revelation of unstable oscillators in the individual presomitic mesoderm cells. *Proc. Natl. Acad. Sci. U. S. A.* 103, 1313–1318.
- Morimoto, M., Takahashi, Y., Endo, M., Saga, Y., 2005. The Mesp2 transcription factor establishes segmental borders by suppressing Notch activity. *Nature* 435, 354–359.
- Muller, M., v Weizsacker, E., Campos-Ortega, J.A., 1996. Expression domains of a zebrafish homologue of the *Drosophila* pair-rule gene *hairy* correspond to primordia of alternating somites. *Development* 122, 2071–2078.
- Nicolas, J.F., Mathis, L., Bonnerot, C., Saurin, W., 1996. Evidence in the mouse for self-renewing stem cells in the formation of a segmented longitudinal structure, the myotome. *Development* 122, 2933–2946.
- Nikaido, M., Kawakami, A., Sawada, A., Furutani-Seiki, M., Takeda, H., Araki, K., 2002. Tbx24, encoding a T-box protein, is mutated in the zebrafish somite-segmentation mutant fused somites. *Nat. Genet.* 31, 195–199.
- Oates, A.C., Ho, R.K., 2002. *Hairy/E(spl)*-related (*Her*) genes are central components of the segmentation oscillator and display redundancy with the Delta/Notch signaling pathway in the formation of anterior segmental boundaries in the zebrafish. *Development* 129, 2929–2946.
- Oates, A.C., Mueller, C., Ho, R.K., 2005. Cooperative function of *deltaC* and *her7* in anterior segment formation. *Dev. Biol.* 280, 133–149.
- Palmeirim, I., Henrique, D., Ish-Horowicz, D., Pourquie, O., 1997. Avian *hairy* gene expression identifies a molecular clock linked to vertebrate segmentation and somitogenesis. *Cell* 91, 639–648.
- Pasini, A., Jiang, Y.J., Wilkinson, D.G., 2004. Two zebrafish Notch-dependent *hairy/Enhancer-of-split*-related genes, *her6* and *her4*, are required to maintain the coordination of cyclic gene expression in the presomitic mesoderm. *Development* 131, 1529–1541.
- Plickert, G., Gajewski, M., Gehrke, G., Gausepohl, H., Schlossherr, J., Ibrahim, H., 1997. Automated in situ detection (AISD) of biomolecules. *Dev. Genes Evol.* 207, 362–367.
- Pourquie, O., Tam, P.P., 2001. A nomenclature for prospective somites and phases of cyclic gene expression in the presomitic mesoderm. *Dev. Cell* 1, 619–620.
- Rida, P.C., Le Minh, N., Jiang, Y.J., 2004. A Notch feeling of somite segmentation and beyond. *Dev. Biol.* 265, 2–22.
- Sawada, A., Fritz, A., Jiang, Y.J., Yamamoto, A., Yamasu, K., Kuroiwa, A., Saga, Y., Takeda, H., 2000. Zebrafish Mesp family genes, *mesp-a* and *mesp-b* are segmentally expressed in the presomitic mesoderm, and Mesp-b confers the anterior identity to the developing somites. *Development* 127, 1691–1702.
- Sieger, D., Tautz, D., Gajewski, M., 2003. The role of *Suppressor of Hairless* in Notch mediated signalling during zebrafish somitogenesis. *Mech. Dev.* 120, 1083–1094.
- Sieger, D., Tautz, D., Gajewski, M., 2004. *her11* is involved in the somitogenesis clock in zebrafish. *Dev. Genes Evol.* 214, 393–406.
- Sieger, D., Ackermann, B., Winkler, C., Tautz, D., Gajewski, M., 2006. *her1* and *her13.2* are jointly required for somitic border specification along the entire axis of the fish embryo. *Dev. Biol.* 293, 242–251.
- Takebayashi, K., Akazawa, C., Nakanishi, S., Kageyama, R., 1995. Structure and promoter analysis of the gene encoding the mouse helix–loop–helix factor HES-5. Identification of the neural precursor cell-specific promoter element. *J. Biol. Chem.* 270, 1342–1349.
- Takke, C., Campos-Ortega, J.A., 1999. *her1*, a zebrafish pair-rule like gene, acts downstream of notch signalling to control somite development. *Development* 126, 3005–3014.
- Takke, C., Dornseifer, P., v Weizsacker, E., Campos-Ortega, J.A., 1999. *her4*, a zebrafish homologue of the *Drosophila* neurogenic gene *E(spl)*, is a target of NOTCH signalling. *Development* 126, 1811–1821.
- Turner, D.L., Weintraub, H., 1994. Expression of achaete-scute homolog 3 in *Xenopus* embryos converts ectodermal cells to a neural fate. *Genes Dev.* 8, 1434–1447.
- van Eeden, F.J., Granato, M., Schach, U., Brand, M., Furutani-Seiki, M., Haffter, P., Hammerschmidt, M., Heisenberg, C.P., Jiang, Y.J., Kane, D.A., et al., 1996. Mutations affecting somite formation and patterning in the zebrafish, *Danio rerio*. *Development* 123, 153–164.
- van Eeden, F.J., Holley, S.A., Haffter, P., Nusslein-Volhard, C., 1998. Zebrafish segmentation and pair-rule patterning. *Dev. Genet.* 23, 65–76.
- Weinberg, E.S., Allende, M.L., Kelly, C.S., Abdelhamid, A., Murakami, T., Andermann, P., Doerre, O.G., Grunwald, D.J., Riggleman, B., 1996. Developmental regulation of zebrafish MyoD in wild-type, no tail and spadetail embryos. *Development* 122, 271–280.
- Weizsäcker, E., 1994. Molekulargenetische Untersuchungen an sechs Zebrafisch-Genen mit Homologie zur *Enhancer of split* Gen-Familie von *Drosophila*. PhD thesis, University of Cologne.
- Westin, J., Lardelli, M., 1997. Three novel *Notch* genes in zebrafish: implications for vertebrate *Notch* gene evolution and function. *Dev. Genes Evol.* 207, 51–63.